Brown, D.C.
The Bundle Adjustment - progress and prospects
International Archives of Photogrammetry 21(3) 1976
Paper number 3-03, 33 pages

INTRODUCTION

This paper is an update of an earlier review (Brown (1974)) entitled: *Evolution, Application and Potential of the Bundle Method of Photogrammetric Triangulation* presented two years ago to the Symposium in Stuttgart sponsored by Commission III of ISP. Because of its rather great length, the review was not published in full in the Proceedings of the Symposium but is available on request from DBA Systems. In the present paper the highlights of the development of the bundle method will first be addressed. This will be followed by a review of some recent applications of the bundle method at DBA, the results of which may prove to have significant impact on future design of aerial mapping cameras. Finally, the writer shall put forward some personal opinions on certain aspects of the likely future development of the bundle method.

DEVELOPMENT OF THE BUNDLE METHOD

By 1960 the foundations of the modern bundle method had been laid. It had been shown in Brown (1958), (1959) that the general normal equations for the adjustment of an unrestricted block generated by any combination of unbiased photogrammetric measurements (plate coordinates) or parameters (elements of exterior orientation or coordinates of ground control) is of the basic form

$$(1)\qquad \begin{bmatrix} \dot{N}+\dot{W} & \bar{N} \\ \bar{N}^T & \ddot{N}+\ddot{W} \end{bmatrix} \begin{bmatrix} \dot{\delta} \\ \ddot{\delta} \end{bmatrix} = \begin{bmatrix} \dot{c}-\dot{W}\dot{\epsilon} \\ \ddot{c}-\ddot{W}\ddot{\epsilon} \end{bmatrix} ,$$

in which for a block of m photos containing n measured points in object space

$\dot{\delta}$ = $6m$x1 vector of corrections to elements of exterior orientation $(\alpha,\omega,\kappa,X^c,Y^c,Z^c)$;

$\ddot{\delta}$ = $3n$x1 vector of corrections to coordinates of object points (X,Y,Z);

$\dot{W}$ = $6m$x$6m$ inverse of covariance matrix of elements of exterior orientation;

$\ddot{W}$ = $3n$x$3n$ inverse covariance matrix of coordinates of object points;

$\dot{\epsilon}$ = $6n$x1 vector of discrepancies between a priori (or observed) values of elements of exterior orientation and corresponding values used in linearization of projective equations;

$\ddot{\epsilon}$ = $3n$x1 vector of discrepancies between a priori (or observed) values of coordinates of measured object points and corresponding values used in linearization of projective equations;

$\dot{N},\bar{N},\ddot{N},\dot{c},\ddot{c}$ = contributions to normal equations resulting solely from measured plate coordinates of images.

For moderate to large photogrammetric blocks the feasibility of a practical numerical solution was shown in the above references to hinge on the assumption

of block diagonality of the inverse covariance matrices $\dot{W}$ and $\ddot{W}$, for when these matrices are of the respective forms

$$
\begin{aligned}
\underset{(6m,6m)}{\dot{W}} &= \operatorname{diag}\left(\underset{(6,6)}{\dot{W}_1} \; \underset{(6,6)}{\dot{W}_2} \cdots \underset{(6,6)}{\dot{W}_m} \right) \\
\underset{(3n,3n)}{\ddot{W}} &= \operatorname{diag}\left(\underset{(3,3)}{\ddot{W}_1} \; \underset{(3,3)}{\ddot{W}_2} \cdots \underset{(3,3)}{\ddot{W}_m} \right)
\end{aligned} \tag{2}
$$

the general system of normal equations assumes the following fine structure

$$
\left[\begin{array}{cccc|cccc}
\dot{N}_1 + \dot{W}_1 & 0 & \cdots & 0 & \bar{N}_{11} & \bar{N}_{12} & \cdots & \bar{N}_{1n} \\
0 & \dot{N}_2 + \dot{W}_2 & \cdots & 0 & \bar{N}_{21} & \bar{N}_{22} & \cdots & \bar{N}_{2n} \\
\vdots & \vdots & & \vdots & \vdots & \vdots & & \vdots \\
0 & 0 & \cdots & \dot{N}_m + \dot{W}_m & \bar{N}_{m1} & \bar{N}_{m2} & \cdots & \bar{N}_{mn} \\
\hline
\bar{N}_{11}^T & \bar{N}_{21}^T & \cdots & \bar{N}_{m1}^T & \ddot{N}_1 + \ddot{W}_1 & 0 & \cdots & 0 \\
\bar{N}_{12}^T & \bar{N}_{22}^T & \cdots & \bar{N}_{m2}^T & 0 & \ddot{N}_2 + \ddot{W}_2 & \cdots & 0 \\
\vdots & \vdots & & \vdots & \vdots & \vdots & & \vdots \\
\bar{N}_{1n}^T & \bar{N}_{2n}^T & \cdots & \bar{N}_{mn}^T & 0 & 0 & \cdots & \ddot{N}_n + \ddot{W}_n
\end{array}\right]
\left[\begin{array}{c} \dot{\delta}_1 \\ \dot{\delta}_2 \\ \vdots \\ \dot{\delta}_m \\ \hline \ddot{\delta}_1 \\ \ddot{\delta}_2 \\ \vdots \\ \ddot{\delta}_n \end{array}\right]
=
\left[\begin{array}{c} \dot{c}_1 - \dot{W}_1 \dot{\varepsilon}_1 \\ \dot{c}_2 - \dot{W}_2 \dot{\varepsilon}_2 \\ \vdots \\ \dot{c}_m - \dot{W}_m \dot{\varepsilon}_m \\ \hline \ddot{c}_1 - \ddot{W}_1 \ddot{\varepsilon}_1 \\ \ddot{c}_2 - \ddot{W}_2 \ddot{\varepsilon}_2 \\ \vdots \\ \ddot{c}_n - \ddot{W}_n \ddot{\varepsilon}_n \end{array}\right] \tag{3}
$$

in which

$\dot{\delta}_i$ = 6x1 vector of corrections to elements of exterior orientation of i^{th} photo,

$\ddot{\delta}_j$ = 3x1 vector of corrections to coordinates of j^{th} object point,

$\dot{\varepsilon}_i$ = 6x1 subvector of $\dot{\varepsilon}$ corresponding to i^{th} photo,

$\ddot{\varepsilon}_j$ = 3x1 subvector of $\ddot{\varepsilon}$ corresponding to j^{th} point,

and

$$
\begin{aligned}
\dot{N}_i &= \sum_{j=1}^{n} \dot{N}_{ij} \,, \quad \dot{c}_i = \sum_{j=1}^{n} \dot{c}_{ij} \,, \\
\ddot{N}_j &= \sum_{i=1}^{m} \ddot{N}_{ij} \,, \quad \ddot{c}_j = \sum_{i=1}^{m} \ddot{c}_{ij}
\end{aligned} \tag{4}
$$

The terms $\dot{N}_{ij}, \ddot{N}_{ij}, \bar{N}_{ij}, \dot{c}_{ij}, \ddot{c}_{ij}$ all appear in the following indeterminate subsystem of normal equations

$$
\underset{(6,6)}{\dot{N}_{ij}} \quad \underset{(6,3)}{\bar{N}_{ij}} \quad \underset{(6,1)}{\dot{\delta}_i} = \underset{(6,1)}{\dot{c}_{ij}}
$$
$$
\underset{(3,6)}{\bar{N}_{ij}^T} \quad \underset{(3,3)}{\ddot{N}_{ij}} \quad \underset{(3,1)}{\ddot{\delta}_j} = \underset{(3,1)}{\ddot{c}_{ij}} \tag{5}
$$

which in turn is generated exclusively by the pair of projective equations corresponding to the image of point j on photo i. These elements in (5) are defined by the expressions

$$
\begin{aligned}
\dot{N}_{ij} &= \dot{B}_{ij}^T \; W_{ij} \; \dot{B}_{ij} \,, \quad \dot{c}_{ij} = \dot{B}_{ij}^T \; W_{ij} \; \varepsilon_{ij} \,, \\
\bar{N}_{ij} &= \dot{B}_{ij}^T \; W_{ij} \; \ddot{B}_{ij} \,, \\
\ddot{N}_{ij} &= \ddot{B}_{ij}^T \; W_{ij} \; \ddot{B}_{ij} \,, \quad \ddot{c}_{ij} = \ddot{B}_{ij}^T \; W_{ij} \; \varepsilon_{ij} \,.
\end{aligned} \tag{6}
$$

in which W_{ij} is the inverse of the covariance matrix the measured plate coordinates x_{ij}^0, y_{ij}^0 and the remaining matrices are defined directly by the linearized pair of projective equations generated by x_{ij}^0, y_{ij}^0, namely:

$$
\underset{(2,1)}{v_{ij}} + \underset{(2,6)}{\dot{B}_{ij}} \; \underset{(6,1)}{\dot{\delta}_i} + \underset{(2,3)}{\ddot{B}_{ij}} \; \underset{(3,1)}{\ddot{\delta}_j} = \underset{(2,1)}{\varepsilon_{ij}} \,. \tag{7}
$$

As it stands, the general system of normal equations (3) applies implicitly to the situation wherein all measured points appear on all photos, as may occur in typical terrestrial applications. By contrast, in the case of the typical aerial block a given point will appear on only a relatively small number of photos, usually no more than six for normal side overlap of less than 50 percent. Here, most of the $\bar{N}_{ij}$ submatrices will be null matrices, for $\bar{N}_{ij}$ is nonzero only when the j^{th} point appears on the i^{th} photo (this also applies to the submatrices $\dot{N}_{ij}, \ddot{N}_{ij}, \dot{c}_{ij}, \ddot{c}_{ij}$). Accordingly, for the normal aerial block the overall $\bar{N}$ submatrix will tend to be sparse, as is illustrated in Figure 1 which depicts the coefficient matrix of the general system of normal equations generated by the 4x5 photo block illustrated in Figure 2. It is this characteristic sparseness of $\bar{N}$ coupled with the block diagonality of $\dot{N}+\dot{W}$ and $\ddot{N}+\ddot{W}$ that makes it ultimately practical to solve the system of normal equations for blocks having a moderate to large number of photos.

APPROACHES TO THE SOLUTION OF THE NORMAL EQUATIONS

Even when $\bar{N}$ is not sparse (i.e., most points appear on most photos) the general system of normal equations of order $(6m+3n)\text{x}(6m+3n)$ can easily be reduced to an equivalent system of $6m\text{x}6m$ through the direct elimination of the $\ddot{\delta}$ vector from (1). This leads to the reduced system

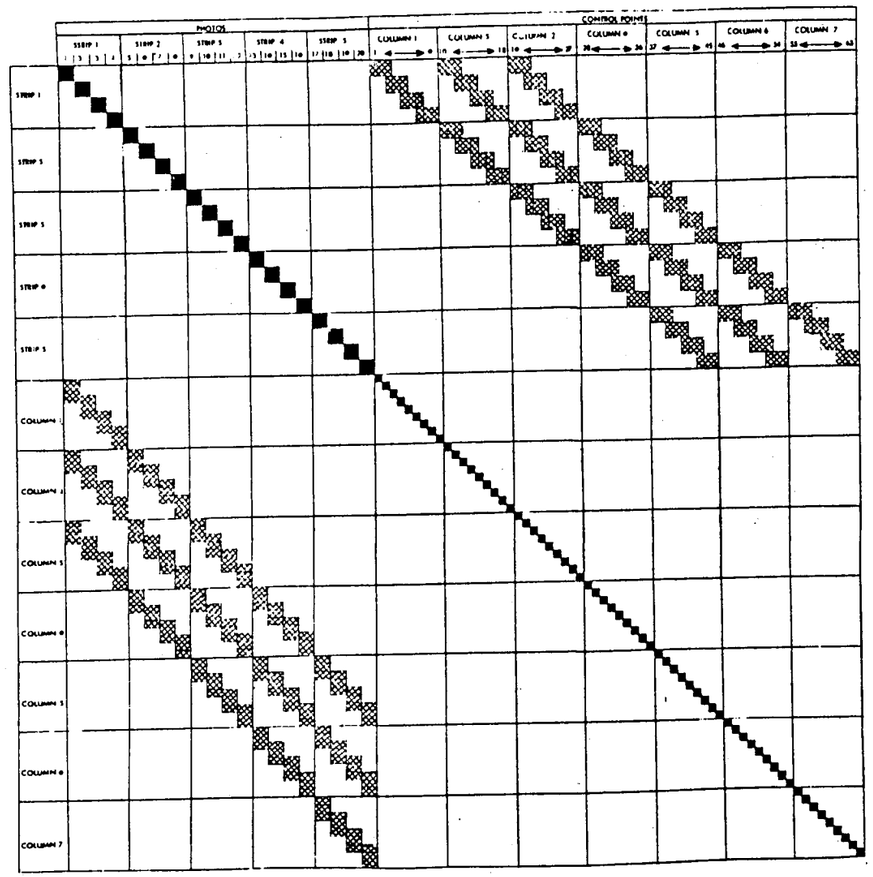

a. Full coefficient matrix.

b. Collapsed matrix.

FIGURE 1. Structure of general normal equations from bundle adjustment of 4x5 photo block of Figure 2 (from Brown, Davis, Johnson (1964)).

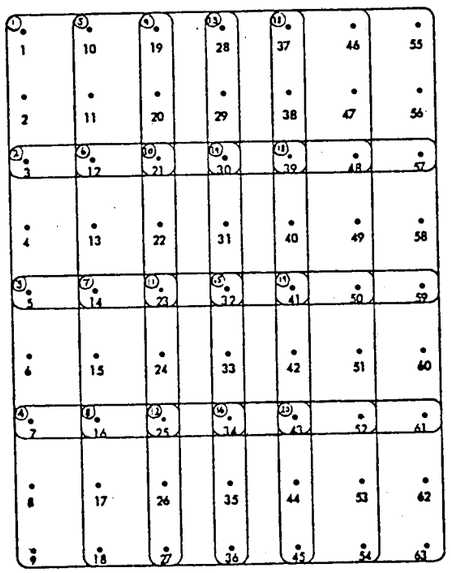

FIGURE 2. Illustrating regular 4x5 block with cross-strip ordering of photos and points.

$$[\dot{N} + \dot{W} - \bar{N}(\ddot{N}+\ddot{W})^{-1}\bar{N}^T]\,\dot{\delta} = \dot{c} - \dot{W}\dot{\varepsilon} - \bar{N}(\ddot{N}+\ddot{W})^{-1}(\ddot{c} - \ddot{W}\ddot{\varepsilon}) \tag{8}$$

involving only elements of orientation as unknowns. The crucial consideration in the formation of the reduced system is that by virtue of the block diagonality of $\ddot{N}+\ddot{W}$ in (1), the required inversion of $\ddot{N}+\ddot{W}$ (a $3n$x$3n$ matrix) reduces to the inversion of n, 3x3 matrices, the $\ddot{N}_i+\ddot{W}_i$. As shown in Brown (1958), by exploiting this fact one can develop the following algorithm for the formation of the reduced normal equations. In terms of the submatrices generated by the j^{th} point in equation (5), the following five auxiliaries are set up

$$\dot{N}_j = \begin{bmatrix} \dot{N}_{1j} & 0 & \cdots & 0 \\ 0 & \dot{N}_{2j} & \cdots & 0 \\ \vdots & \vdots & & \vdots \\ 0 & 0 & \cdots & \dot{N}_{nj} \end{bmatrix}, \quad \bar{N}_j = \begin{bmatrix} \bar{N}_{1j} \\ \bar{N}_{2j} \\ \vdots \\ \bar{N}_{nj} \end{bmatrix}, \quad \dot{c}_j = \begin{bmatrix} \dot{c}_{1j} \\ \dot{c}_{2j} \\ \vdots \\ \dot{c}_{nj} \end{bmatrix} \tag{9}$$

$$\ddot{N}_j = \sum_{i=1}^{n} \ddot{N}_{ij}, \qquad \ddot{c}_j = \sum_{i=1}^{n} \ddot{c}_{ij} \tag{10}$$

In terms of these and the quantities $\ddot{W}_j, \ddot{\varepsilon}_j$ the following secondary auxiliaries are evaluated

$$\begin{aligned} Q_j &= (\ddot{N}_j + \ddot{W}_j)^{-1}\,\bar{N}_j^T \\ R_j &= \bar{N}_j\,Q_j \\ S_j &= \dot{N}_j - R_j \\ \bar{c}_j &= \dot{c}_j - Q_j^T(\ddot{c}_j - \ddot{W}_j\ddot{\varepsilon}_j) \end{aligned} \tag{11}$$

As the S and $\bar{c}$ matrices are generated for each point, in turn, they are added to the sums of their antecedents to produce ultimately the quantities

$$\begin{aligned} S &= S_1 + S_2 + \ldots + S_n \\ \bar{c} &= \bar{c}_1 + \bar{c}_2 + \ldots + \bar{c}_n \end{aligned} \tag{12}$$

The desired reduced system of normal equations (8) is then given by

(13) $$(\dot{S}+\dot{W})\,\dot{\delta} = \overline{c} - \dot{W}\dot{\varepsilon} \ .$$

When the number of photos is not excessively large this $6m$x$6m$ system can be solved by standard methods of inversion to yield

(14) $$\dot{\delta} = (S+\dot{W})^{-1}\,(\overline{c} - \dot{W}\dot{\varepsilon}) \ .$$

With the vector of corrections to the elements of orientation thus established, each vector of corrections to the approximate coordinates of object points can be computed sequentially from

(15) $$\ddot{\delta}_j = (\ddot{N}_j+\ddot{W}_j)^{-1}\,(\ddot{c}_j - \ddot{W}_j\ddot{\varepsilon}_j) - Q_j\dot{\delta} \qquad j = 1,2,\ldots,n.$$

The corrections resulting from (14) and (15) may be employed to generate refined approximations, thus initiating an iterative process that can be carried to convergence. Thereupon, the covariance matrix $\dot{\Lambda}$ of the adjusted elements of orientation and the covariance matrix $\ddot{\Lambda}_j$ of the adjusted coordinates of the j^{th} point can be evaluated from

(16) $$\dot{\Lambda} = (S+\dot{W})^{-1} \ ,$$

(17) $$\ddot{\Lambda}_j = (\ddot{N}_j + \ddot{W}_j)^{-1} + Q_j\,\dot{\Lambda}\,Q_j^T \ .$$

The above development provided the basis for the practical utilization of the bundle adjustment in the early 1960's. In applications involving relatively small numbers of photographs (e.g., terrestrial applications) the solution of the reduced system of normal equations presented no practical difficulties; here, a straightforward process of Gaussian elimination was altogether adequate. However, in applications to aerial blocks the direct solution of the reduced system of normal equations by standard methods became increasingly impractical with increasing numbers of photos and was clearly unfeasible (even with large and advanced computers) for blocks containing many hundreds of photos. The first practical resolution of this basic difficulty was developed in Brown, Davis and Johnson (1964). Here, specific advantage was taken of the characteristic sparseness of the $\overline{N}$ submatrix associated with aerial blocks. Instead of operating on the reduced system of normal equations (8), Brown, Davis and Johnson reverted to the general system (3) and instead of attempting to effect a direct solution of this system, they employed the indirect method of Block Successive Over-Relaxation (BSOR). The effectiveness of this approach depended on the use of an indexing scheme whereby (a) only the nonzero submatrices of the normal equations would be formed and (b) these would be stored and operated on in a collapsed form as illustrated in Figure 1b. By eliminating all superfluous operations on zero matrices this process drastically reduced storage requirements, and greatly facilitated the formation and solution (by BSOR) of the normal equations. As a consequence, by 1966 it became practical to adjust blocks containing more than 1000 photos by means of the operational computer program implementing the 'collapsed' BSOR reduction (Davis 1965)).

The BSOR approach suffered from two primary shortcomings. The first was that the number of iterations required for satisfactory convergence turned out to be rather sensitive to the quantity and distribution of absolute control throughout the block — the more control, the faster the convergence. With minimal or sparse control slowness of convergence could detract significantly from the otherwise satisfactory efficiency of the reduction. The second shortcoming of the BSOR approach was that it did not produce the inverse of the coefficient matrix of the normal equations. As a result, the computation of the covariance matrices of the triangulated coordinates could not be accomplished efficiently.

Because of the shortcomings of the BSOR reduction the search for greater computational efficiency continued. The next advance occurred in late 1965 with the development at DBA of an algorithm named *recursive partitioning*. This algorithm, first published in Gyer (1967), is designed expressly to exploit the characteristic banded structure of the reduced normal equations generated by the typical aerial block with appropriately ordered photos. This banded structure is illustrated in Figure 3 for a sequence of blocks conforming to the cross-strip ordering scheme indicated in Figure 2. With such ordering all nonzero elements of the coefficient matrix are confined to a diagonal band the width of which depends only on the number of strips in the block (for a particular degree of side overlap) and is totally independent of the number of photos per strip.

Recursive Partitioning is applicable not only to banded systems but also to banded-bordered systems having the structure indicated in Figure 4 which depicts an NxN coefficient matrix having bandwidth p and borderwidth q. As shall be seen in due course, the availability of the band in this system affords diverse opportunities for the practical extension of the basic bundle adjustment to accommodate the introduction of parameters common to significant subsets of photos. As adopted from Brown (1968a) a concise explanation of the process of recursive partitioning proceeds as follows. One begins with the quadruply partitioned banded-bordered system of bandwidth p and borderwidth q indicated below.

(18)

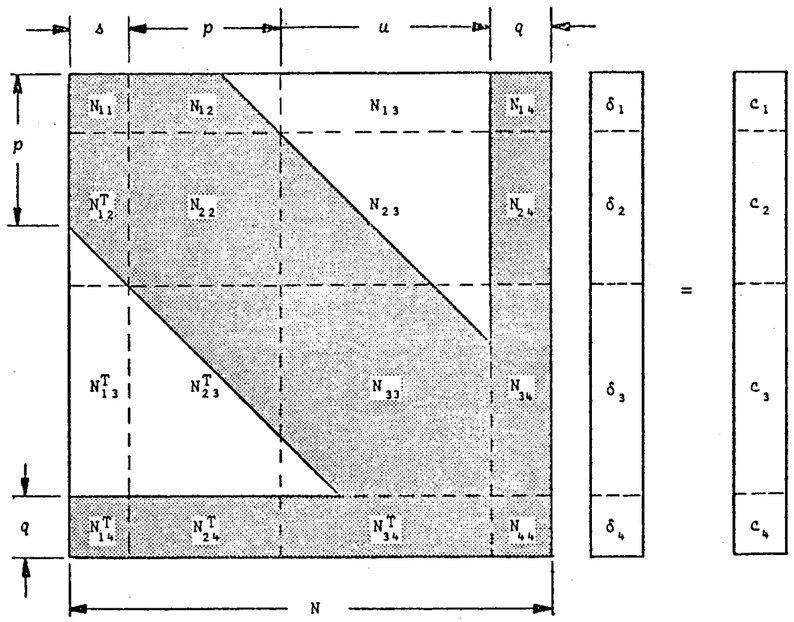

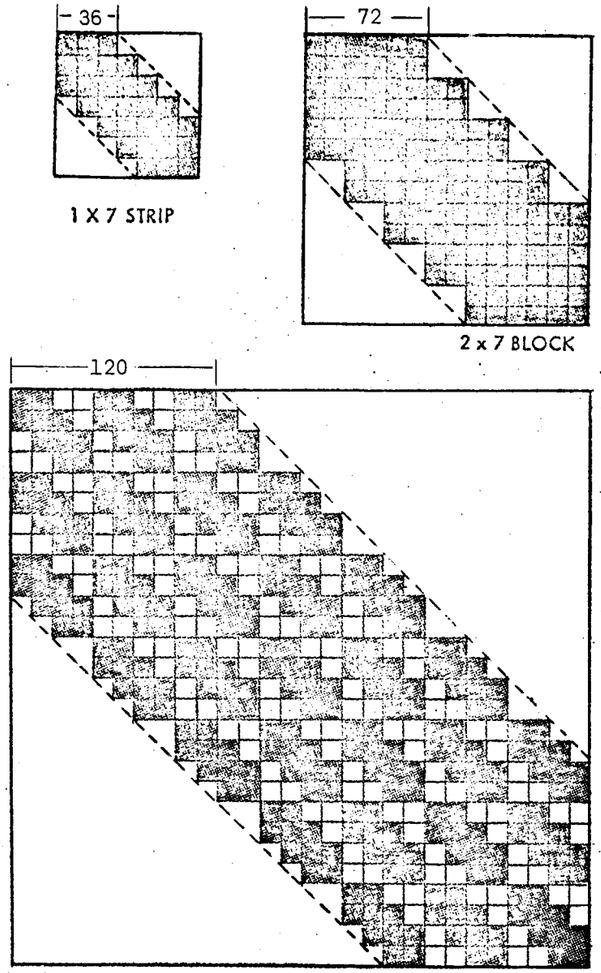

FIGURE 3. Illustrating banded structure of reduced system of normal equations resulting from bundle-adjustment of a succession of regular blocks having strip ordering as in Figure 2.

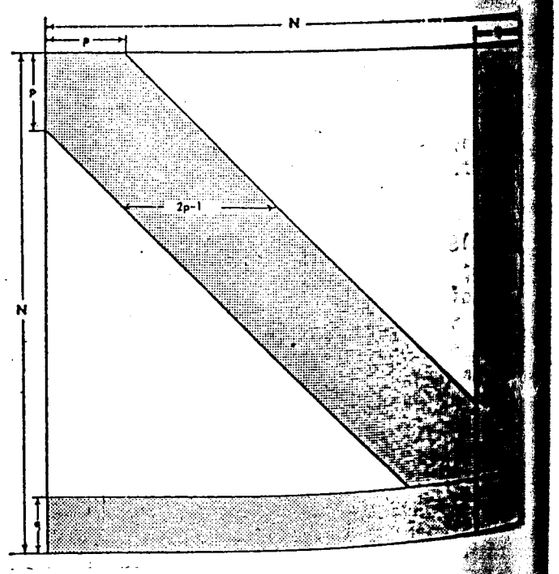

FIGURE 4. Illustrating form of NxN banded-bordered coefficient matrix with bandwith p and borderwidth q.

The number of elements δ in the first partition is arbitrary except that $\delta = p$, the bandwidth. The number of elements in the second partition is equal to the bandwidth p. The number of elements in the third partition is $u = N - (\delta + p + q)$, which automatically leaves in the last partition a number of elements equal to the borderwidth q. By virtue of this partitioning the submatrices N_{13} and N_{13}^T are composed entirely of zeroes. By formally applying the method of partitioning to eliminate the subvector δ_1 from the above system, one obtains

$$(19)\quad \left\{ \begin{bmatrix} N_{22} & N_{23} & N_{24} \\ N_{23}^T & N_{33} & N_{34} \\ N_{24}^T & N_{34}^T & N_{44} \end{bmatrix} - \begin{bmatrix} N_{12}^T \\ N_{13}^T \\ N_{14}^T \end{bmatrix} N_{11}^{-1} \begin{bmatrix} N_{12} & N_{13} & N_{14} \end{bmatrix} \right\} \begin{bmatrix} \delta_2 \\ \delta_3 \\ \delta_4 \end{bmatrix} = \begin{bmatrix} c_2 \\ c_3 \\ c_4 \end{bmatrix} - \begin{bmatrix} N_{12}^T \\ N_{13}^T \\ N_{14}^T \end{bmatrix} N_{11}^{-1} c_1$$

But because N_{13}, N_{13}^T are zero matrices by deliberate construction, this reduces immediately to

$$(20)\quad \begin{bmatrix} N_{22} - N_{12}^T N_{11}^{-1} N_{12} & N_{23} & N_{24} - N_{12}^T N_{11}^{-1} N_{14} \\ N_{23}^T & N_{33} & N_{34} \\ N_{24}^T - N_{14}^T N_{11}^{-1} N_{12} & N_{34}^T & N_{44} - N_{14}^T N_{11}^{-1} N_{14} \end{bmatrix} \begin{bmatrix} \delta_2 \\ \delta_3 \\ \delta_4 \end{bmatrix} = \begin{bmatrix} c_2 - N_{12}^T N_{11}^{-1} c_1 \\ c_3 \\ c_4 - N_{14}^T N_{11}^{-1} c_1 \end{bmatrix}$$

By comparing this reduced system with the starting system (18), one sees that the essential banded-bordered form of the original coefficient matrix is preserved with bandwidth p and borderwidth q remaining unaltered. Within the original band of the matrix the following changes occur: N_{11}, N_{12}, N_{12}^T are eliminated and their influence is absorbed (or folded) into N_{22} which is the only surviving portion of the band to be altered (N_{33}, N_{23}, N_{23}^T are unaffected by the operation). In the original border N_{14}, N_{14}^T are eliminated, having been folded into N_{24}, N_{24}^T and N_{44}; the remainder of the border N_{34}, N_{34}^T is unaltered. Because the foregoing procedure results in no change whatever in the basic structure of the coefficient matrix (only the overall dimensions are changed from NxN to $(N-\delta)x(N-\delta)$), it is clear that one could quadrupally partition the reduced matrix and then repeat the process of elimination. At no stage of the repeated application of this process would one ever operate outside the original band or border. Moreover, at any step of the process only the four matrices corresponding to the current N_{22}, N_{24}, N_{24}^T and N_{44} are subject to alteration. The overall process thus constitutes a simple repetitive reduction that can be formulated as a recurrent (or recursive) process and hence the designation *recursive partitioning*. Repeated application of the reduction will ultimately lead to a system sufficiently small to be solved directly for all the remaining unknowns. These can then be used to initiate a backward application of the process wherein the unknowns eliminated at each step of the forward process are recovered in reverse order. As in the forward reduction, bandwidth and borderwidth are strictly preserved. The number of arithmetic operations required for the reduction of an NxN banded-bordered system of bandwidth p and borderwidth q is, for $p>>q$ (which is generally the case in practical applications), approximately proportional to $(p+q)^2N$ as compared with a number proportional to N^3 in a conventional reduction by procedures akin to Gaussian elimination. Thus enormous computational savings

are possible when $(p+q) << N$ as is often the case with large photogrammetric blocks.

As shown in Gyer (1967) recursive partitioning can also be employed to generate only that portion of the inverse enveloped by the band and border of the original matrix. The computer time required for this reduction is approximately twice the time required for the solution alone. This development made feasible the performance of the rigorous analytical error propagation associated with the coordinates of the triangulated points. It also permitted the recovery of the covariance matrix of the additional parameters carried in the reduction. This, in turn, provides a rational basis for judging the significance and separability of the additional parameters.

The first practical implementation of recursive partitioning for banded systems in a bundle adjustment program occurred in late 1966 at DBA. Here, the existing bundle adjustment incorporating BSOR was appropriately modified to accommodate recursive partitioning in place of BSOR. In a demonstration of the program in January 1967 a 162 photo block (9 strips of 16 photos) was reduced in 210 minutes on DBA's relatively modest CDC-3100 computer which had only 8K of memory (48 bit words), 4 magnetic tape units, no disc files and no floating point hardware. Extrapolated to one of the most powerful computers available at that time, the CDC-6600, the time to be expected for the same reduction would have been well under two minutes. As a result of this demonstration, DBA received a contract change from Rome Air Development Center (RADC) to implement recursive partitioning in the BSOR block adjustment program then under development for use on the GE 635 computer at RADC. By May 1967 recursive partitioning had been implemented on the GE 635 and during that month a number of tests employing simulated blocks were run. The testing culminated with the adjustment of a 1000 photo block consisting of 5 strips of 200 photos. The entire reduction was accomplished in 40 minutes for a single pass.

In November 1967 complete documentation of the GE 635 program, which later became named SURBAT (*Simultaneous, Unlimited, Rigorous Block Analytical Triangulation*), was published in Gyer, Lewis, Saliba (1967). SURBAT was set up to process as many as 50 strips with an unlimited number of photographs per strip (if required, this was expandable to a maximum of 450 strips through changes in dimension statements). The program made provisions for automatic editing and for the execution of the rigorous error propagation associated with the triangulation. Being the first large scale operational program for bundle adjustment to benefit fully from the enormous efficiencies attendant on the incorporation of recursive partitioning, SURBAT may be said to have brought the bundle adjustment to basic maturity in practical applications to aerial triangulation.

THEORY OF SELF-CALIBRATION WITH INTERNAL AND EXTERNAL OBSERVATIONS

Although SURBAT and its proprietary companion program at DBA, COMBAT (*COmmercial Block Analytical Triangulation*), made large scale bundle adjustments economically feasible, they fell short of implementing the full theoretical base that had already been developed at DBA. In Brown, Davis, Johnson (1964) the theory of the bundle had been developed to accommodate the possibility that any of the quantities entering the adjustment could be subject not only to random errors but also to systematic error describable by appropriate analytical error models. A specific example cited in this reference to illustrate the basics of the approach considered a situation in which auxiliary sensors consisting of an inertial navigation system and a statoscope were employed in conjunction with an aerial mapping camera. Corresponding to the j^{th} exposure on the i^{th} strip and under the assumption of essentially constant

flying velocity along the strip, these sensors were assumed to introduce auxiliary observational equations of the form

$$\underset{\substack{(adjusted\\ value)}}{\phi_{ij}} - \underset{\substack{(observed\\ value)}}{\phi^0_{ij}} = \underset{(residual)}{v_{\phi_{ij}}} + \underbrace{a_{0i} + a_{1i}\tau_{ij} + a_{2i}\sin\frac{2\pi}{P}\tau_{ij} + a_{3i}\cos\frac{2\pi}{P}\tau_{ij} + \cdots}_{Error\ Model}$$

$$\underset{\substack{(adjusted\\ value)}}{\lambda_{ij}} - \underset{\substack{(observed\\ value)}}{\lambda^0_{ij}} = \underset{(residual)}{v_{\lambda_{ij}}} + \underbrace{b_{0i} + b_{1i}\tau_{ij} + b_{2i}\sin\frac{2\pi}{P}\tau_{ij} + b_{3i}\cos\frac{2\pi}{P}\tau_{ij} + \cdots}_{Error\ Model}$$

$$\underset{\substack{(adjusted\\ value)}}{h_{ij}} - \underset{\substack{(observed\\ value)}}{h^0_{ij}} = \underset{(residual)}{v_{h_{ij}}} + \underbrace{c_{0i} + c_{1i}\tau_{ij} + c_{2i}\tau^2_{ij} + \cdots}_{Error\ Model}$$

in which

$\phi_{ij}, \lambda_{ij}, h_{ij}$ = latitude, longitude and height of j^{th} exposure on i^{th} strip;

$\tau_{ij} = t_{ij} - t_{i0}$ = time of exposure ij relative to time t_{i0} arbitrarily adopted to index i^{th} strip;

P = Shuler Period (approximately 84 minutes);

$a_{0i}, a_{1i}, a_{2i}, \cdots$
$b_{0i}, b_{1i}, b_{2i}, \cdots$
$c_{0i}, c_{1i}, c_{2i}, \cdots$
} error coefficients of inertial navigator (a's and b's) and of statoscope (c's).

The coefficients of the error model of the inertial sensor were chosen to reflect the unknown dominant linear drift of the navigational error as modulated by the Schuler period, and the coefficients of the error model for the statoscope were chosen to reflect the unknown but slowly varying departure of the adopted isobaric surface from the reference spheroid along the course of the i^{th} strip. Each of the error coefficients was considered to be subject to appropriate a priori constraints governed by prespecified covariance matrices.

The specialization of the development of Brown, Davis, Johnson (1964) to apply to the particular set of auxiliary sensors considered above leads ultimately to a banded-bordered system of normal equations with the border accommodating the parameters of the auxiliary sensors. As formulated, a fresh set of error parameters could be introduced for each strip or for specified sub-blocks, in which case the border itself would assume a patterned structure subject to special exploitation.

The general development of Brown, Davis, Johnson (1964) constitutes in its broadest form the theory of self-calibration of photogrammetric systems embracing auxiliary sensors affected by possible systematic errors governed by error models of known functional form and having error

coefficients subject to specified a priori constraints. When the plate coordinates themselves are considered to be subject to systematic errors governed by specified error models, the camera simply loses its special status in the above theory and becomes merely one of a set of biased sensors that serve ultimately to interrelate coordinates of sets of ground points.

PRACTICAL IMPLEMENTATION OF SELF-CALIBRATION

The possibility of the practical implementation of the above theory to aerial blocks on a routine basis had to wait for the development some two years later of recursive partitioning of banded-bordered systems. Indeed, the extension of recursive partitioning from banded systems to banded-bordered systems was specifically motivated by the consideration that most potential applications of self-calibration could be expected to lead to the addition of a border on the basic banded system. The earliest actual applications of principles of self-calibration to analytical photogrammetry occurred in terrestrial applications involving only small numbers of photos, for here the solution of the normal equations did not pose a significant problem. In 1965 the longstanding DBA program STEREO, a bundle adjustment which had been designed expressly for applications to structural measurements, was modified to permit the recovery (through self-calibration) of coefficients of radial and decentering distortion as well as elements of interior orientation x_p, y_p, c. This led to most successful results when certain basic geometrical principles were implemented in the field operation (e.g., use of at least three, well-placed exposures having moderate to high convergence and a diversity of swing angles). As a result, in applications to structural measurements it became possible to substitute the on-the-job process of self-calibration for laborious procedures of pre-calibration that had previously been necessary. This permitted accuracies to be achieved ranging routinely from 1 part in 50,000 to 1 part in 100,000 of the major diameter of the photographed structure. Details of such applications of the bundle adjustment with self-calibration to terrestrial photogrammetry are to be found in Kenefick (1971) and Brown (1971),(1972).

As for the routine implementation of self-calibration to blocks of aerial photos, this was to come about much more slowly, even though structural consequences and the newly found practical mechanics of the process (i.e., recursive partitioning of banded-bordered systems) had been disclosed in three separate papers delivered in 1968 (Brown (1968a), (1968b),(1968c)). Although the first actual application of self-calibration to an aerial block was reported in Brown (1968c), the application could hardly be considered routine, for the block was a highly specialized one of 40 photos comprised of two sets of 20 photo blocks, both consisting of a pair of orthogonal flight lines each flown in opposing directions with about 90% overlap on each run of 5 photos. The original intention of the project was to perform an in-flight calibration of an Air Force KC-6A camera from photos taken over the McLure, Ohio, Aerial Test Range which had permanent, presurveyed monuments at fairly regular intervals. In due course, however, it became obvious from analysis of residuals that the accuracy of the survey of the 50 or so available control points was simply not sufficient to permit the points to be enforced. Accordingly, the adjustment was revised so that coordinates of ground points became subject to adjustment along with the measured plate coordinates. This led to an overall set of some 1200 residuals having an rms error of only 2.9μm, but which, as can be seen from Figure 5a, nonetheless displayed definite and

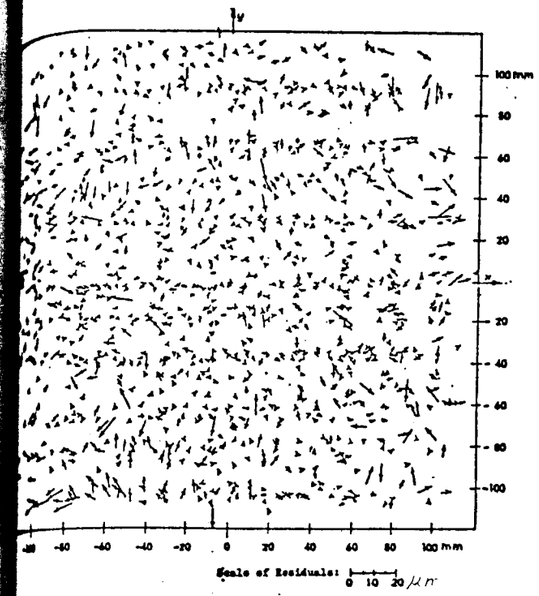

FIGURE 5. Illustrating analysis of residuals from bundle adjustment with self-calibration for determination of anomalous distortion.

a. *(opposite)* Composite plot of residual vectors from 40 frames taken by KC-6A camera over McLure Test Range.

b. *(lower left)* Contour map of x component of anomalous distortion derived from residual vectors.

c. *(lower right)* Contour map of y component of anomalous distortion.

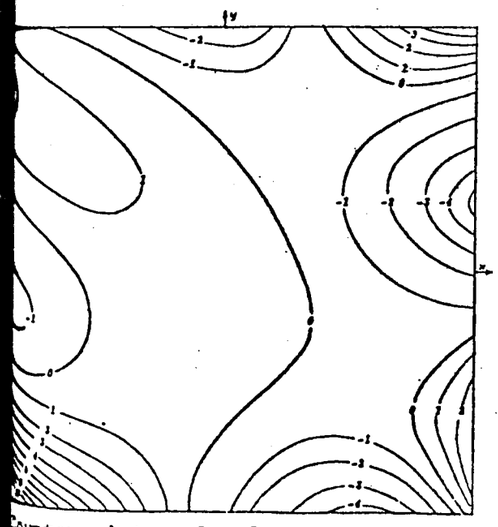

Contour interval = 1 μm.

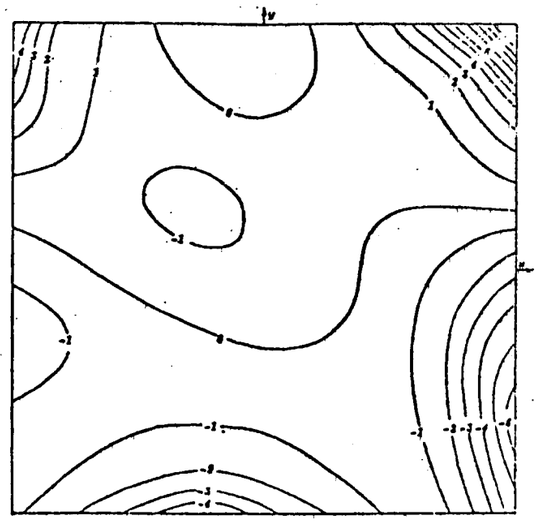

Contour interval = 1 μm.

significant systematic tendencies toward the edges of the format. This was so even though the effects of survey errors had been accounted for along with effects of radial and decentering distortion (by virtue of self-calibration), as well as effects of film deformation (by virtue of the reseau platen incorporated in the camera). The expression *anomalous distortion* was coined to designate this persistent residual systematic error. The x and y components of anomalous distortion as derived from fifth order x,y polynomials fitted to the residuals of Figure 5a are depicted in terms of contour maps in Figures 5b and 5c. In some parts of the format such distortion clearly assumes practical significance. With effects of anomalous distortion removed, the rms value of the revised residuals improved from 2.9μm to 2.3μm. This suggests that attainment of an rms value of 2.0μm from the bundle adjustment with self-calibration may not constitute an unreasonable goal.

Although the McLure project did successfully exercise the concept of self-calibration with an aerial block, it did not exercise recursive partitioning to effect the solution of the reduced system of normal equations. Recursive partitioning was simply not appropriate in this instance inasmuch as the coefficient matrix became almost completely filled because of the particular nature of the block. However, it was clearly pointed out in Brown (1968c) that in applications of the process of self-calibration to more conventional aerial blocks the normal equations would assume a banded-bordered form and thus be amenable to reduction by recursive partitioning.

The first application of the bundle adjustment with self-calibration to a conventional aerial block was reported by Bauer and Müller (1972) who employed a 5x26 photo block taken over the Oberschwaben Test Field. Although only four parameters of the error model could be accommodated at a time in their reduction, Bauer and Müller achieved remarkable improvements in accuracies of triangulation when self-calibration was exercised — almost 300 percent in horizontal coordinates and about 50 percent in vertical coordinates. These concrete results have stimulated widespread interest in the bundle adjustment with self-calibration, as is apparent from many of the papers of the present symposium. Accordingly, a brief review of some recent, previously unreported experiences at DBA with the practical applications of the process is appropriate at this point.

THE VERMONT PROJECT

The Vermont Project employed a block of some 264 photos in 15 strips as shown in Figure 6 which also depicts the layout of the ground control available for the project. The following further specifications are pertinent:

Date of Photography: *May 1974*
Camera: *Zeiss RMK A 8.5/23 (Super Wide Angle)*
Camera Platen: *Special 61-point reseau platen designed and fabricated by DBA*
Photographic Scale: *1:62,500*
Mean Flying Height above Terrain: *17,500 ft.*
Forward Overlap: *60%*
Side Overlap: *60%*

A primary objective of the project was the tenfold densification of the existing horizontal geodetic survey from about 40 monumented points (largely on mountain tops) to about 400 monumented points (mainly near roads in

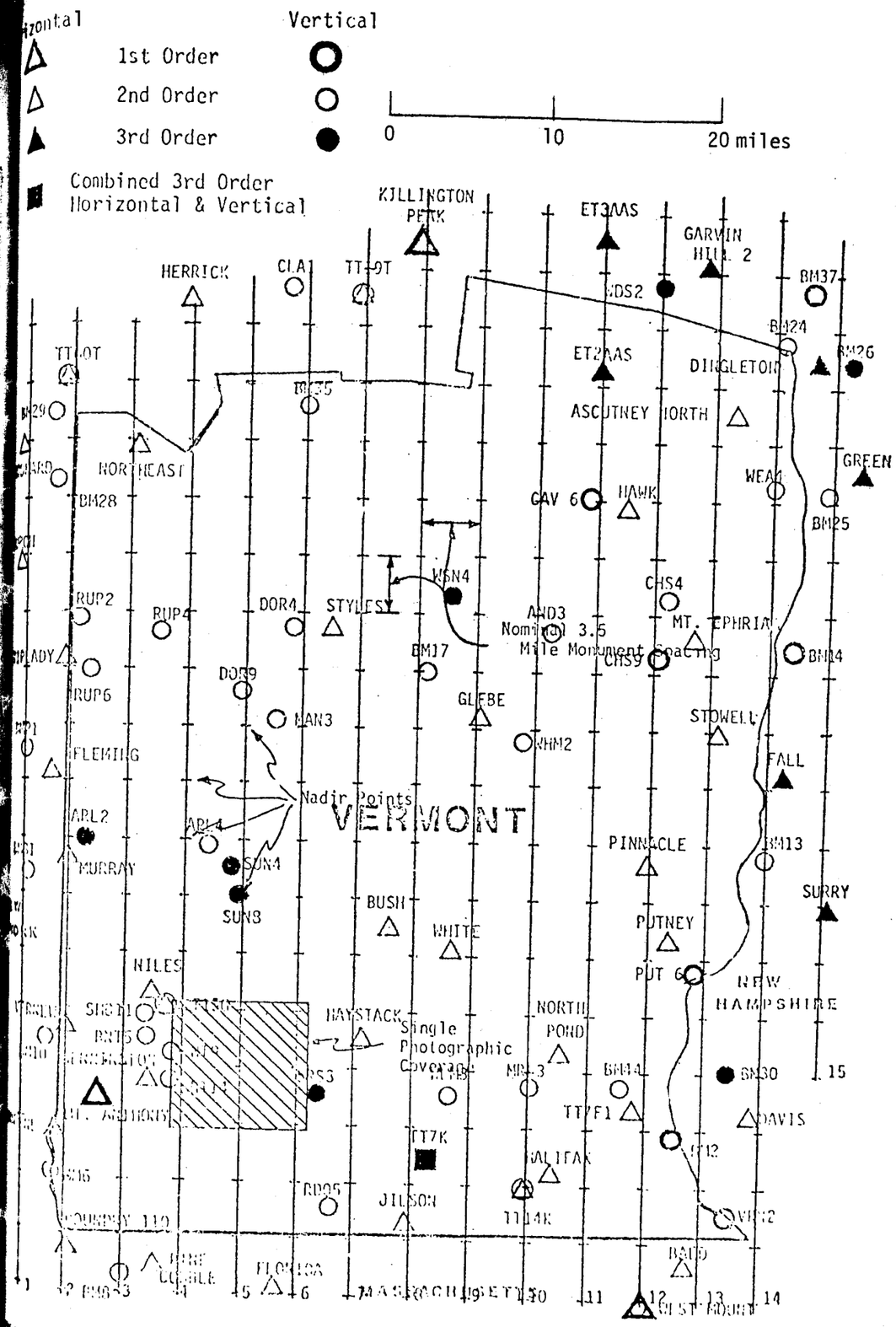

FIGURE 6. Layout of Vermont Project.

valleys insofar as practicable). Though of secondary interest, vertical densification was also to be accomplished.

As previously reported (Brown (1973),(1974)) the error model employed at the time in the DBA program Combat II contained 29 terms and was of the form:

$$\begin{aligned}\Delta x = {} & a_1 x + a_2 y + a_3 x^2 + a_4 xy + a_5 y^2 + a_6 x^2 y + a_7 xy^2 \\ & + \frac{x}{c}(c_1 x^2 + c_2 xy + c_3 y^2 + c_4 x^3 + c_5 x^2 y + c_6 xy^2 + c_7 y^3) \\ & + x(K_1 r^2 + K_2 r^4 + K_3 r^6) \\ & + P_1(y^2 + 3x^2) + 2P_2 xy \\ & + \delta x_p + \left(\frac{x}{c}\right)\delta c \end{aligned} \tag{22}$$

$$\begin{aligned}\Delta y = {} & b_1 x + b_2 y + b_3 x^2 + b_4 xy + b_5 y^2 + b_6 x^2 y + b_7 xy^2 \\ & + \frac{y}{c}(c_1 x^2 + c_2 xy + c_3 y^2 + c_4 x^3 + c_5 x^2 y + c_6 xy^2 + c_7 y^3) \\ & + y(K_1 r^2 + K_2 r^4 + K_3 r^6) \\ & + 2P_1 xy + P_2(x^2 + 3y^2) \\ & + \delta y_p + \left(\frac{y}{c}\right)\delta c. \end{aligned}$$

in which the various coefficients may be interpreted in groups to correspond to the following:

(a) $a_1, a_2, \ldots, a_7$ } empirical coefficients defining combination of
$b_1, b_2, \ldots, b_7$ } mean uncompensated film deformation and anomalous distortion;

(b) $c_1, c_2, \ldots, c_7$: coefficients defining curvature or unflatness of platen;

(c) K_1, K_2, K_3: coefficients of radial distortion;

(d) P_1, P_2: coefficients of decentering distortion;

(e) δx_p, δy_p, c: biases in enforced elements of interior orientation.

Being a 'raw' mixed empirical and analytical model, the above formulation can be expected to suffer from strong correlations between various parameters. However, as the writer explained in discussions at the 1974 Stuttgart

Symposium, problems of ill-conditioning are circumvented by the following procedure:

(i) first, apriori reasoning may be invoked to suppress certain parameters at the outset: for example, those in group (e) would never be exercised with normal vertical photography over flat to moderate terrain because of their almost perfect coupling with coordinates of the exposure stations; on the other hand, they may be held in reserve for possible application in special circumstances warranting their exercise (e.g., with highly convergent photographs);

(ii) in an initial reduction, each parameter to be provisionally exercised may be regarded as having an apriori value of zero governed by an arbitrary, rather loose apriori variance (chosen, for example, to allow the term involving the parameter to assume a maximum absolute value of perhaps 100μm within the format);

(iii) by virtue of the imposition of the aforementioned loose apriori constraints, determinacy of the initial reduction is assured and the covariance matrix of the adjusted error parameters can be evaluated;

(iv) from the correlation matrix generated from the covariance matrix those terms that are inherently inseparable in the problem at hand will immediately be evident by virtue of their very high correlations (typically on the order of .99);

(v) of each pair (or group) of coefficients exhibiting excessively high correlation, all but an arbitrarily selected one can justifiably be suppressed (through exercise of tight apriori variances) in a repetition of the reduction.

Carried to completion, the above process leads rather automatically to a reduced set of separable parameters and avoids problems with ill-conditioning. As applied to the Vermont block, it led to the suppression of the following coefficients (in addition to the presuppressed $\delta x_p, \delta y_p, \delta c$): $a_3, a_6, b_1, b_2, b_5, c_1, c_2, c_5, K_1, P_1, P_2$.

Of the 46 available horizontal control points shown in Figure 6 only 3 were of first order accuracy while 35 and 8, respectively, were of second and third order accuracy. The apriori standard deviations assigned to the three respective classes of control points were: 0.5 ft., 1.0 ft., and 3.0 ft. The bundle adjustment was executed both with and without the exercise of self-calibration. In both reductions, all control points were carried in the adjustment subject to the just mentioned apriori constraints. The most remarkable results of the comparative reductions are those presented in Table 1 which lists the horizontal corrections developed for each control point by each of the two reductions. One sees that the corrections arising from the bundle adjustment without self-calibration are decidedly large in comparison with their apriori standard deviations and are strongly systematic. With second order control points, for instance, the Root Mean Square (RMS) values of the corrections in X and Y are 4.9 ft. and 3.9 ft., respectively, as compared with the assigned, apriori one sigma value of 1.0 ft. (at plate scale the corrections amount to 24 and 19 μm, respectively). This, of course, is indicative of the presence of a severe internal strain in the

TABLE 1. Corrections obtained for horizontal control points from bundle adjustment with and without self-calibration.

POINT	CORRECTIONS With Self-Cal. ΔX (ft)	With Self-Cal. ΔY (ft)	Without Self-Cal. ΔX (ft)	Without Self-Cal. ΔY (ft)
First Order (a priori σ=0.5)				
Killington	-0.1	-0.6	1.0	2.7
West Mount	0.0	-0.2	-0.5	-6.6
Mt.Anthony	-0.2	0.1	1.3	-1.7
RMS:	0.1	0.4	1.0	4.2
Second Order (a priori σ=1.0)				
Stoddard	0.2	0.2	6.0	0.9
Burch	-0.4	-2.3	5.0	-8.4
TTGOT	1.7	0.8	11.2	5.3
Tiplady	0.9	0.2	9.1	-3.4
Fleming	-1.1	0.1	7.9	-3.3
Murray	0.8	-0.5	9.2	-2.0
Vernew	-0.2	-1.1	4.6	-1.9
Greene	-1.7	0.8	-0.9	-1.0
Boundary	0.3	0.2	-0.5	-4.8
Herrick	0.0	2.4	6.7	7.4
Northeast	0.3	-0.9	5.9	0.0
Niles	-0.7	-0.2	2.1	1.4
TTISG	-0.2	-0.3	2.6	-1.5
Bennington	0.0	-0.6	0.9	-3.5
Pine Cobble	0.0	0.6	-1.9	-5.4
TT19T	-1.8	2.4	0.3	6.7
Styles	0.1	-1.1	1.9	-1.7
Bush	0.1	-0.7	0.5	-2.8
Haystack	-0.1	0.1	-0.3	-1.7
Florida	-0.6	1.4	-3.7	-5.5
Second Order (continued)				
Globe	0.9	-0.1	-0.2	1.5
White	0.4	-0.8	-0.7	-3.9
Jilson	0.0	0.9	-3.4	-6.7
Ascutney	-0.4	0.7	-5.2	6.2
Hawk	0.4	0.2	-3.4	4.2
Mt.Ephriam	-1.3	-1.5	-6.8	0.7
Stowell	-0.6	-0.7	-7.1	1.0
Pinnacle	-0.2	-0.2	-5.0	1.4
Putney	0.2	0.5	-4.9	0.2
North Pond	3.0	2.1	1.7	2.1
TT7FI	0.4	-1.6	-3.2	-4.0
TT14K	0.8	-0.4	-1.1	-5.6
Halifax	1.4	0.1	-0.6	-4.5
Davis	-1.6	0.3	-9.4	0.4
Bald	-0.6	0.2	-2.1	-1.0
RMS:	0.9	1.0	4.9	3.9
Third Order (a priori σ=3.0)				
ET3AAS	3.2	3.7	3.0	11.7
ET2AAS	-0.5	3.5	-3.0	9.6
Garvin Hill	0.1	0.2	-1.3	7.9
Dingleton	-0.2	3.2	-0.5	9.5
Green	0.4	-3.4	-6.6	-1.2
Fall	-4.0	0.4	-14.4	0.6
Surry	1.3	0.1	-7.1	2.1
TT7K	1.1	1.5	-1.3	-5.6
RMS:	1.9	2.5	6.4	7.2

adjustment caused, in turn, by a significant degree of uncompensated systematic error. By contrast, when the bundle adjustment with self-calibration is performed, the internal strain is entirely removed and the RMS values of the X,Y corrections for second order points become 0.9 and 1.0 ft., respectively (or 4.4 and 4.9 μm at plate scale) — a four to fivefold improvement over the results without self-calibration. Generally comparable improvements were also obtained for vertical coordinates; details are not presented here because the summary of the vertical corrections without self-calibration had been misplaced and could not be located at the time of this writing. However, results for vertical corrections are at hand for the reduction with self-calibration; here, the RMS value of the vertical corrections turned out to be 0.5 ft, or 2.4 μm at plate scale.

Because self-calibration yielded such dramatic improvements, it is of major interest to ascertain which parameters of the error model were mainly responsible for the favorable outcome. As it turned out, of the fifteen error coefficients that were actually exercised only five or six were found to be significantly different from zero and, of these, the totally dominant terms were those describing symmetric radial distortion. This was indeed a major surprise, for the precalibrated distortion function had been duly and correctly applied to generate appropriate corrections to the plate coordinates prior to the adjustment. Hence, the coefficients

radial distortion resulting from the process of self-calibration should have ideally been insignificantly different from zero. Instead, these coefficients alone yielded corrections amounting to a-difficult-to-accept value of 30 μm at a radial distance of 140 mm. Moreover, it turned out that these coefficients could not be suppressed in repetitions of the bundle adjustment without severely degrading the results. Therefore, the effects had to be regarded as having a real physical basis. To explain the phenomenon the following hypothesis emerged. The results could be attributed to an actual physical change in the lens itself due to the extreme coldness of the air outside the airplane at the average flying altitude of 6000 meters above mean sea level (over Vermont in mid May). This resulted in a pronounced temperature gradient between the front and rear elements of the lens, thus altering the distortion of the lens to the value recovered by the bundle adjustment with self-calibration. The large diameters of the front and rear elements of the super wide angle lens tended to support the plausibility of the argument. At the time, the writer was quite satisfied with the thermal gradient hypothesis. However, it was incorrect, as the consequences of the project in Atlanta were subsequently to establish.

THE ATLANTA PROJECT

In March 1975 a small block of 28 photos in 4 strips was flown over the City of Atlanta in a pilot project to test the practicability of photogrammetric densification of geodetic nets in an urban environment. Atlanta is heavily wooded in residential areas and is quite hilly, thus making it a rather dubious candidate for photography taken by a super wide angle camera. Nonetheless, the same Zeiss RMK A 8.5/23 camera as was used in the Vermont Project was also used in the Atlanta Project, one specific objective of the test being to determine the operational suitability of the super wide angle camera in urban applications to densification. The choice of the super wide angle mapping camera (f=85 mm), rather than the more conventional wide angle mapping camera (f=150 mm), was governed by the following well-known considerations. When both cameras are flown at the same scale, they yield essentially equivalent accuracies in planimetry. However, because of its more favorable base/height ratio, the super wide angle camera can *theoretically* be expected to produce heights that are nearly twice as accurate as those produced by a wide angle mapping camera. This means that once the accuracy for height has been specified, a wide angle camera must be flown at twice the scale as a super wide angle mapping camera in order to produce equivalent accuracies in height; this in turn means that the photographic block generated by the former will contain four times as many photos as the block generated by the latter. Accordingly, in theory at least, the super wide angle camera enjoys an enormous potential economic advantage over the normal wide angle camera. The problem has been that the theoretical advantage of the super wide angle camera seems rarely, if ever, to have been realized in practice. Investigations reported in Ackermann (1974a) indicate vertical accuracies of the super wide angle camera actually to be inferior to those of the wide angle camera for photography of the same scale. Presumably, this shortfall is attributable to systematic errors that, hopefully, could be removed by the process of self-calibration. Another objective of the Atlanta Project, then, was to establish whether or not this is the case.

The Atlanta Project was a joint effort of DBA Systems and Airborne Data Inc. in conjunction with the City of Atlanta and the Georgia Department of Transportation (DOT) all operating under the auspices of the

Georgia Coordinate Mapping Committee. A major responsibility of DOT was to spot check the accuracies of the photogrammetric results by means of independent ground surveys. The project encompassed a 3x4 mile area as shown in Figure 7. At nominal half mile intervals within this area potential locations for permanent monuments were selected — a total of 63 locations in all. Actual locations of monuments were established by field reconnaissance to be as close as possible to the ideal locations laid out on a map. As can be seen from Figure 7 which depicts the actual locations of the monuments, it turned out to be possible to adhere rather closely to the planned layout despite the wooded, hilly and built-up character of the landscape. Near each of the selected locations of the monuments two circular targets of 32 inch diameter were painted in fluorescent orange along the center of the adjacent roadway. The separation of the targets was preset to be precisely 30 feet and the center of each target was marked by a surveyor's nail. The monument itself, whether actual or potential (some were put in after the photography), was located off the roadway along the nominal perpendicular bisector of the line joining the two painted targets as shown in Figure 8. In those cases where monuments were actually implanted, the offset distances of the monument from the centers of the two painted targets were measured along with the differences in height between the monument and the centers of the targets. From these easily made offset measurements and the coordinates (ultimately to be established photogrammetrically) of the neighboring targets it becomes a simple matter to compute the precise coordinates of the monument itself. This means that the permanent monument need not actually be installed prior to the photography — it can be installed at any desired later time as long as the centers of the associated offset targets remain recoverable. This constitutes a significant advantage of the offset target method, for the installation of monuments is a far more time consuming and tedious task than the painting of dual targets in the roadway. Moreover, because of the designed proximity of each eventual monument to corresponding pairs of painted monuments, the necessary offset measurements can be made quickly, easily and inexpensively by relatively unskilled personnel. Two other advantages of this approach are noteworthy: vandalism of movable targets placed over monuments is a major problem in urban areas, whereas targets painted in the roadway are virtually immune to disruption; and such targets are less likely than the monument itself to be obscured in the photography by nearby trees or structures.

In addition to the 63 pairs of offset targets just discussed, a total of 32 painted, single targets was established close to the boundary of the block to serve as *wing pass points* to help strengthen the photogrammetric adjustment. Horizontal control was provided by six paneled, first order points indicated in Figure 7. With the exception of the station Pershing vertical control coincided with horizontal control. In addition to this vertical control, a single vertical point (DOT 32) was especially established near the center of the block by the Georgia DOT.

Photographic coverage of the test area was taken at a scale of 1 : 17,500 (altitude ~ 4900 ft) with DBA's Zeiss RMK A 8.5/23 camera using, as in Vermont, the DBA 61 point reseau platen. With both forward and side overlap of 60%, each photo contained a rather uniform pattern of 25 points (or pairs of points). The photographs proved to be of excellent quality. Moreover, none of the painted targets was obscured. This demonstrated that near optimal distribution of targets is altogether practical in an urban area even when photography is performed with a super wide angle camera and thus answered one of the questions raised before the test.

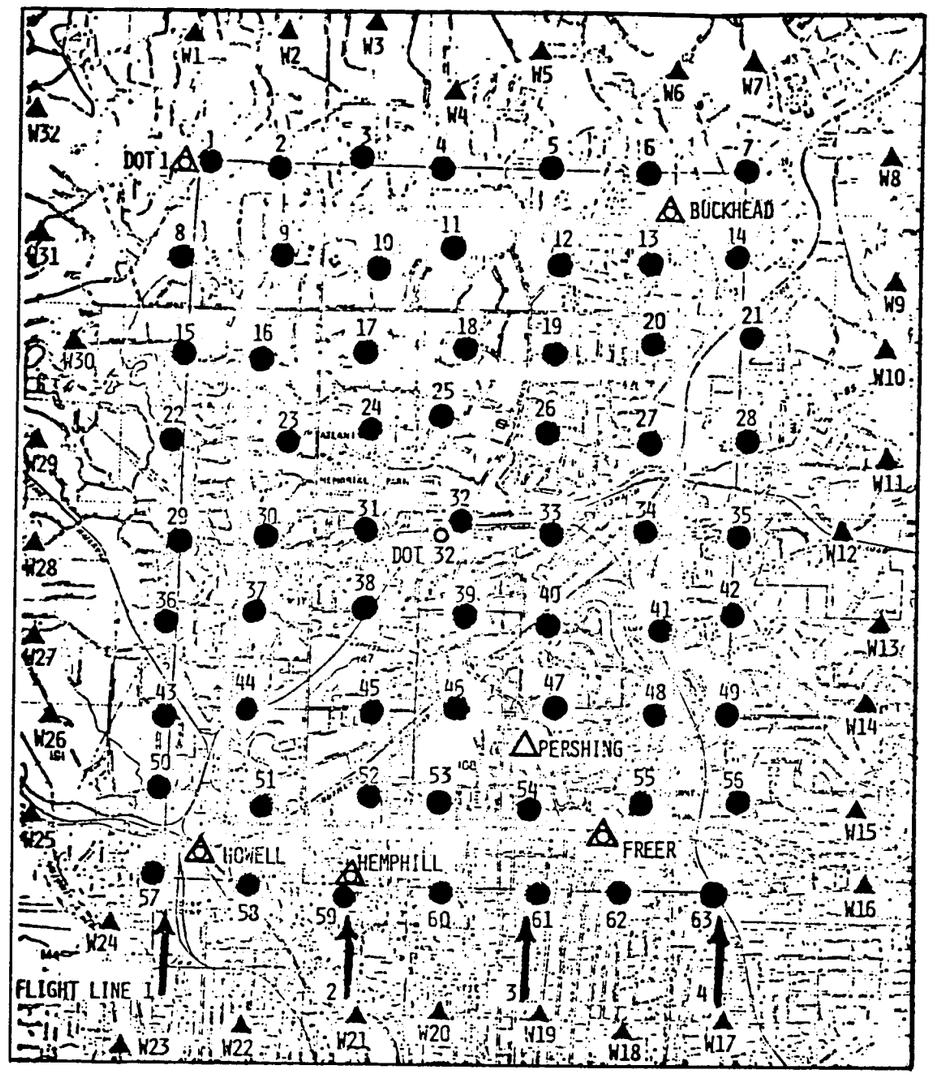

FIGURE 7. Layout of Atlanta Project.

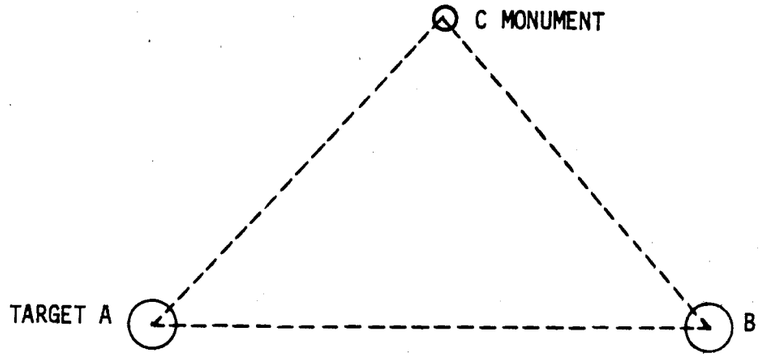

FIGURE 8. Illustrating process of location of monument by means of measurements from nearby offset targets. Distance AB between centers of offset targets is pre-established to a convenient fixed value (30 ft in the Atlanta Project). Monument C is located approximately equidistant from A and B and subtends an angle close to the optimum value of 90°. After monument has been so installed, distances BC and AC are taped and height differences between A and C and B and C are measured. From these quantities together with the photogrammetrically determined coordinates of A and B the coordinates of the monument can be computed.

TABLE 2. Discrepancies at checkpoints of Atlanta Project.

		POINT	MEAN DISCREPANCIES (ft) ΔX (East)	ΔY (North)	ΔZ (Up)
HORIZONTAL CHECKPOINTS	OFF TARGETS	10A	-.524	.022	-
		10B	-.572	.098	-
		11A	.507	.011	-
		11B	.037	-.240	-
		12A	.155	.151	-
		12B	.205	.011	-
		18A	.111	.321	-
		18B	.387	.340	-
		39A	-.111	.007	-
		39B	.018	-.515	-
		41A	.069	-.032	-
		41B	-.229	-.198	-
		RMS:	.310 ft (5.4μm)*	.226 ft (3.9μm)*	-
	MONUMENTS	10	-.459	.141	-
		11	.181	-.077	-
		12	.127	.035	-
		18	.226	.167	-
		39	-.071	-.239	-
		41	-.055	.009	-
		RMS:	.230 ft (4.0μm)*	.136 ft (2.4μm)*	-
VERTICAL CKPTS	OFF TAR	34A	-	-	.031
		34B	-	-	.141
		39A	-	-	-.298
		39B	-	-	.046
		47A	-	-	.018
		47B	-	-	.060
		RMS:	-	-	.139 ft (2.4μm)*
	MON	34	-	-	.081
		39	-	-	-.127
		47	-	-	.049
		RMS:	-	-	.091 ft (1.6μm)*

* At plate scale

In the bundle adjustment of the block of 28 photos the same subset of error coefficients was exercised as in the Vermont Project. Surprisingly, the resulting systematic corrections turned out to be very similar to those obtained in the Vermont Project. In particular, a large correction for radial distortion was obtained, as is clear from Figure 9 which presents a vector plot over the format of the recovered systematic corrections. This demolished the 'thermal gradient' hypothesis advanced earlier, for very nearly the same radial distortion function was recovered in the Atlanta Project, even though the camera was subject to much more moderate variations of temperature because of the lower flying altitude. Accordingly, it became necessary to seek another explanation, a topic that will be addressed shortly.

After completion of the photogrammetric reduction DBA sent the coordinates of all of the offset targets to the Georgia DOT. Also sent were the coordinates of all installed monuments as computed by DBA from the necessary offset measurements supplied by the Public Works Department of the City of Atlanta. After receiving the final coordinates from DBA, the Georgia DOT made a selection of the points to be field checked and conducted the necessary surveys. A total of 18 horizontal checks were made by means of a first order traverse. These corresponded to six triplets, each consisting of two painted targets and the associated monument. In addition, a total of nine vertical checks (i.e., three triplets) were made

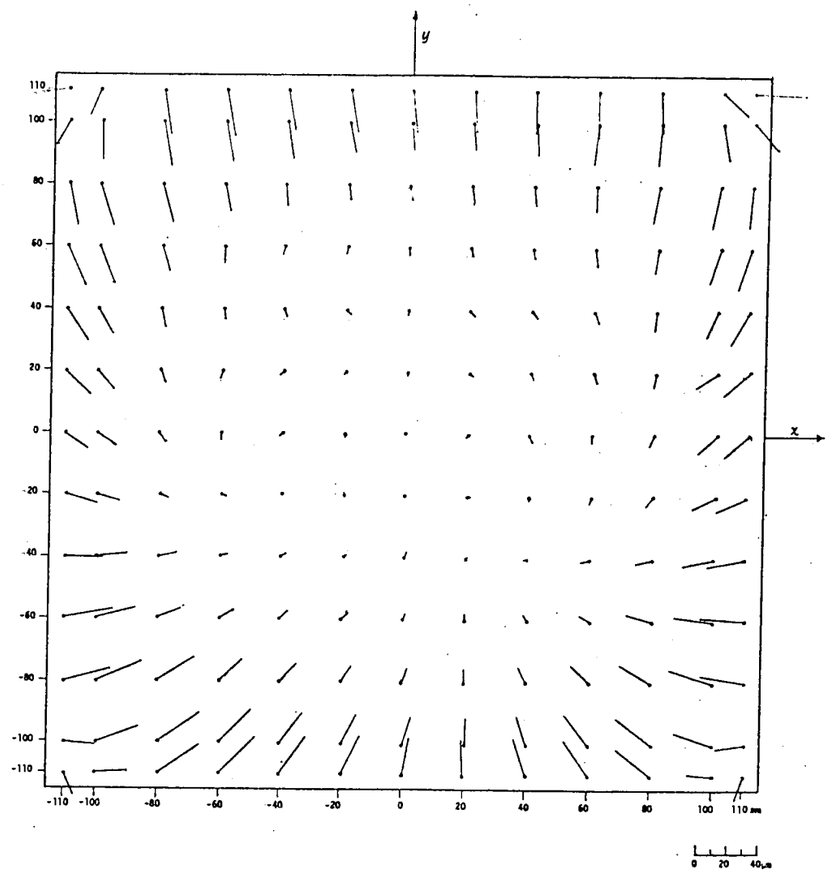

FIGURE 9. Vectors of total systematic corrections recovered by bundle adjustment with self-calibration on Atlanta Project.

by leveling. The discrepancies between the photogrammetric and ground surveys of the check points were computed by the DOT and are summarized in Table 2. Separate breakdowns are given for targets and monuments, for the latter were not triangulated directly, but, as mentioned above, were computed from the coordinates of the targets and the offset measurements.

It is seen from Table 2 that RMS errors for targets at plate scale are 5.4, 3.9 and 2.4 μm in X,Y and Z respectively; for the monuments the corresponding figures are 4.0, 2.4 and 1.6 μm. The relatively higher accuracies obtained for the monuments are consistent with expectations. because errors in the coordinates of the two offset targets are essentially averaged in the reduction leading to the coordinates of the monument (the error in the offset measurements themselves are of no practical significance). With optimal geometry (i.e., monument equidistant from offset targets and subtending a 90° angle), the theoretical improvement in accuracies for the horizontal coordinates of the monument over those of the offset targets is about 25 percent; for the vertical coordinate it is about 30 percent. This, then, constitutes still another advantage of the offset target method.

Because of the smallness of the sample of check points (especially for vertical coordinates) one should not draw overly strong conclusions from the above results. In particular, the extraordinarily good results for vertical accuracies must partially be regarded as fortuitous because they exceed theoretical expectations by almost a factor of two. The analytical error propagation performed in conjunction with the photogrammetric triangulation and carried through the computation of the positions of the monuments yielded the following results: targets, $\sigma_x,\sigma_y \approx .19$ to .24 ft. (3.3 to 4.2 μm at plate scale), $\sigma_z \approx .21$ to .26 ft. (3.7 to 4.5 μm); monuments, $\sigma_x,\sigma_y \approx .14$ to .19 ft. (2.4 to 3.3 μm), $\sigma_z \approx .13$ to 18 ft. (2.3 to 3.1 μm). Except for the overly optimistic outcome for vertical coordinates, results from the check points are seen to be fairly consistent with theoretical expectations. One rather firm conclusion to be drawn from the Atlanta Project is that the potential superiority of the super wide angle camera with regard to accuracies of vertical coordinates can indeed be realized through the use of the bundle adjustment with self-calibration.

INVESTIGATIONS OF FLATNESS OF FILM PLATENS

As mentioned, the hypothesis that the large correction for radial distortion could be explained by thermally induced changes in the lens itself became untenable as a result of the outcome of the Atlanta Project. Accordingly, an alternative explanation had to be sought. Renewed consideration was then given to another possibility that had earlier been dismissed, namely, curvature of the platen. To the degree that such curvature is radially symmetric, it is projectively equivalent to radial distortion. The DBA Reseau Platen used in both the Vermont and Atlanta Projects had been designed to be at least as sturdy as the original Zeiss platen which it was to replace. As measured, following completion of its fabrication, it was extraordinarily flat with an rms departure from a best fitting plane of only 1.5 μm. Following the Vermont Project the platen was remeasured and found to have changed its figure somewhat to an rms departure of 2.6 μm — still exceptionally good and totally inadequate to explain the recovered radial distortion. Following the breakdown of the 'thermal' hypothesis resulting from the Atlanta Project, the platen was once again measured. This time, its rms departure had deteriorated to 5.3 μm and its actual figure was decidedly concave. This still was not enough to explain the matter under investigation, but it did establish a

clear trend of deterioration in the figure of the platen. Normally, such deterioriation might be attributed to the gradual release metallurgical strains, but not in the case at hand, for the DBA platen was made of an alloy called Precedent 71 which has a stability approaching that of fused quartz. Some other physical process had to be involved. At this point, the decision was made to measure the platen with film in place and with the application of the film-flattening vacuum (about 0.1 atmosphere). This vacuum was produced by the pump of the camera itself, for in this way there would be no question concerning the correctness of the degree of the applied vacuum. The results were startling. Relative to one corner of the format, the center of the platen dropped over 20 μm when the vacuum was turned on. A full set of 169 measurements of spot elevations confirmed that a pronounced, systematic change in the figure of the platen had indeed occurred with the application of the film-flattening vacuum. Moreover, the actual figure of the platen under the film-flattening vacuum could fully account for the magnitude of the apparent radial distortion uncovered in the Vermont and Atlanta Projects. Here, then, was the physical explanation that had been sought. The deformation induced by the vacuum also explained the slowly changing static figure of the platen — with continuing use the platen had acquired an increasingly concave 'set' as result of repeated flexing of the surface in response to each application of the vacuum.

Contour maps of the surface of the DBA Reseau Platen resulting from the succession of measurements referred to above are shown in Figure 10. Of especial importance is Figure 10d which indicates the topography of the platen when the normal operating vacuum is applied. It is something close to this geometry that existed when the photographs of the Vermont and Atlanta Projects were taken. One should appreciate, however, that the laboratory measurements may not fully apply to the platen under operating conditions in the camera, for to some extent the figure of the platen may benefit from edge flattening resulting from pressure against the frame defining the focal plane.

The experiments with the DBA Reseau Platen naturally raised related questions concerning the operational stability of the Zeiss platen normally used in the camera. Measurements before and after the application of the vacuum were accordingly made on this platen also. The results given in Figure 11 show that the Zeiss platen is subject to similar deformation from the vacuum. The Zeiss platen seems also to have acquired a concave set from long term use. As can be seen from comparison of Figures 10d and 11b, the contours of the Zeiss platen are more circular than those of the DBA platen which tend to be rather square with rounded corners. These differences reflect the respective geometries of the re-enforcing ribs on the backsides of the two platens — a centrally radiating 'spiderweb' pattern in the case of the Zeiss platen and a 3x4 'box cell' pattern in the case of the DBA platen. Because of the radial symmetry of the ribs of the Zeiss platen, it turns out that a second degree polynomial can provide an excellent analytical representation of the surface, whereas, as can be seen from Table 3, a fourth degree polynomial is needed for a comparable fit to the DBA platen. In the process of polynomial fitting, it appears that terms involving even powers of x and y are dominant (note, for instance, with the DBA platen the trivial improvement of the third degree fit as opposed to the marked improvement with the fourth degree fit). This result is in conformance with what is to be expected from the series solution of the partial differential equation governing the deformation of evenly loaded plates (Sechler (1968)). This consideration is reflected in a revised version of the error model currently used at DBA, a topic to be taken up later.

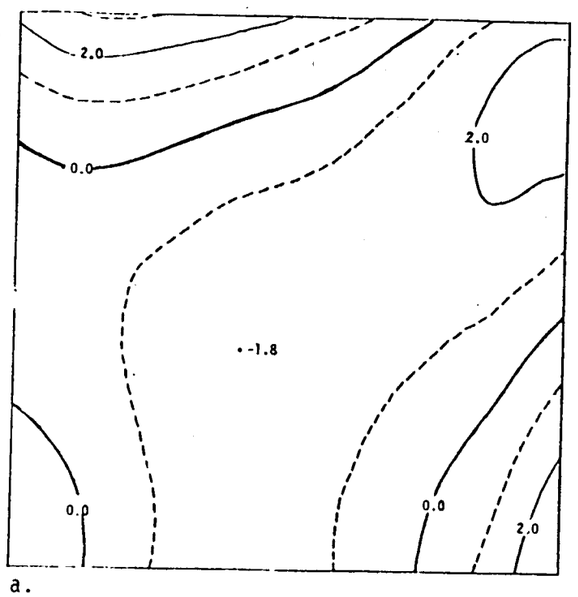

a.

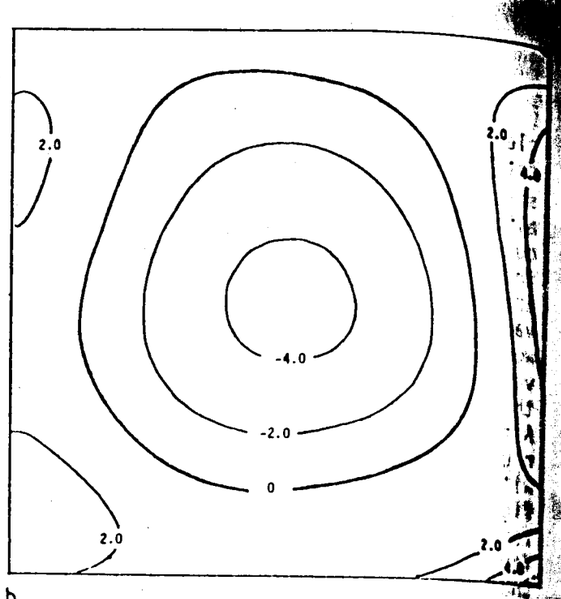

b.

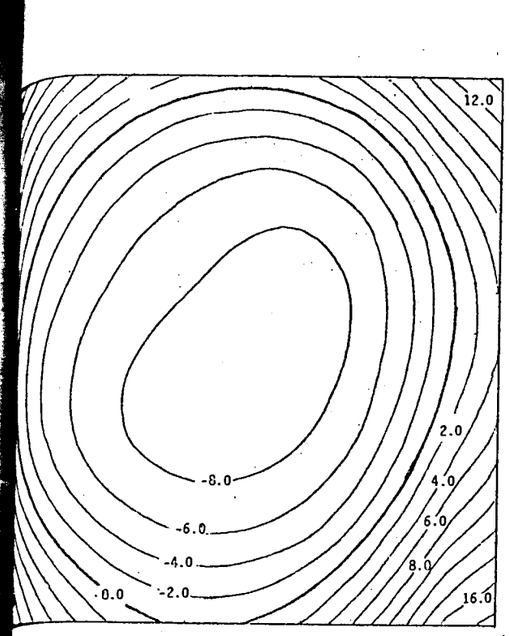

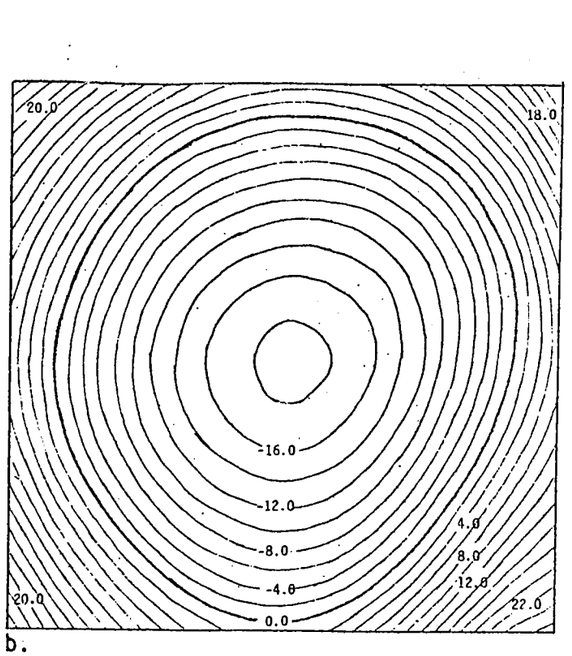

b.

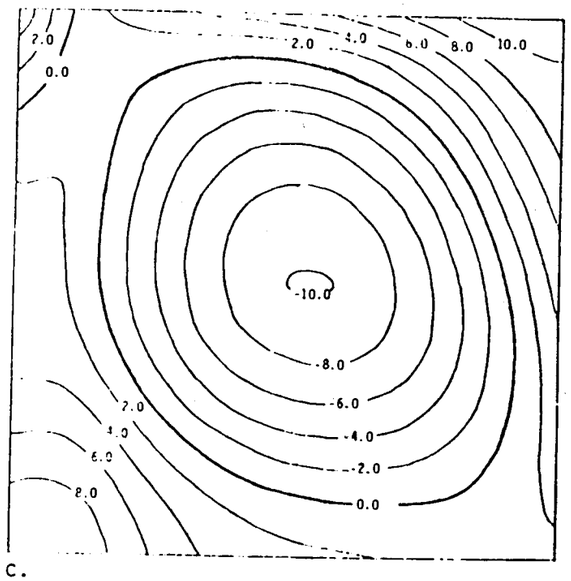

c.

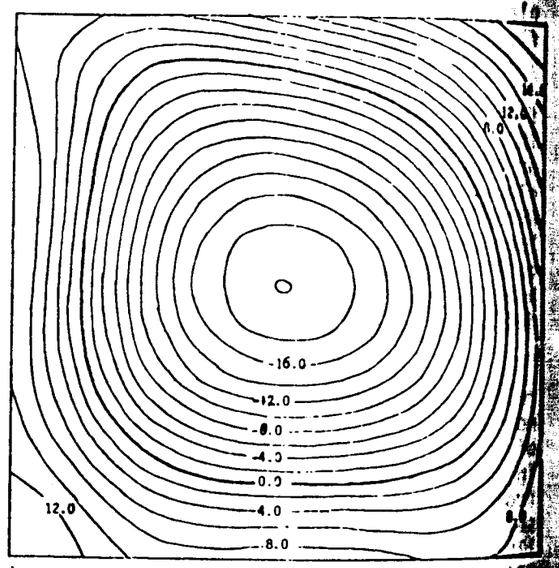

d.

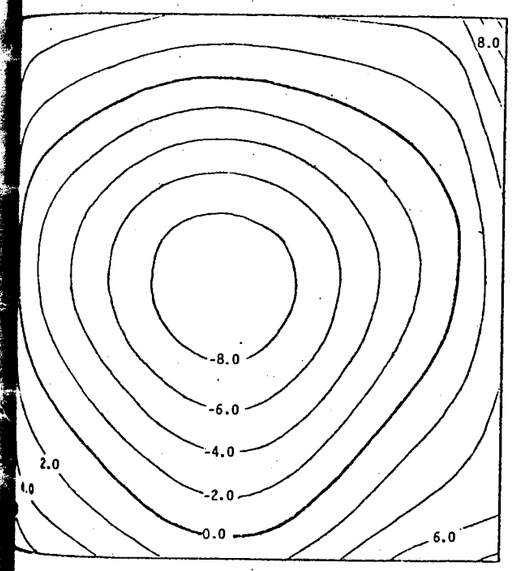

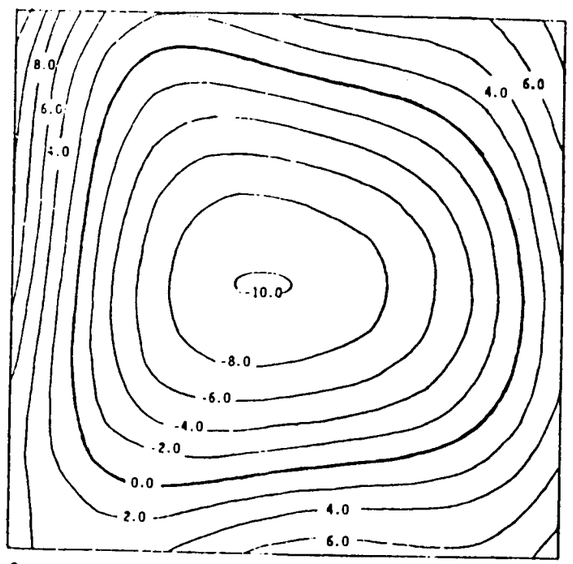

e.

FIGURE 10. Contour maps of original version of DBA reseau platen under various circumstances.

a. after original manufacture, March 1974 *(rms unflatness = 1.5 µm)*

b. after initial use on Vermont Project, June 1974 *(rms unflatness = 2.2 µm)*

c. after Atlanta Project, June 1975 *(rms unflatness = 5.3 µm)*

d. same as c but with application of film-flattening vacuum *(rms unflatness = 10.2 µm)*

e. change in flatness with application of vacuum (difference between d and c).

FIGURE 11. Contour maps of Zeiss platen from super wide angle camera.

a. without application of film-flattening vacuum *(rms unflatness = 7.2 µm)*

b. with application of film-flattening vacuum *(rms unflatness = 11.6 µm)*

c. difference between b and a.

TABLE 3. RMS fit of polynomials of various degree to measurements of spot heights of DBA and Zeiss platens.

Degree	RMS Values of Residuals of Best Fitting Polynomials			
	DBA Reseau Platen		*Zeiss Platen*	
	Vacuum Off	Vacuum On	Vacuum Off	Vacuum On
1	5.27 µm	10.20 µm	7.20 µm	11.58 µm
2	2.28	3.86	1.35	1.56
3	2.13	3.72	1.32	1.44
4	0.99	1.61	1.21	1.24
5	0.81	1.44	1.19	1.17
6	0.78	1.37	0.99	1.14

As a result of the foregoing findings, a completely new version of the DBA Reseau Platen has been designed and fabricated. The design of this platen renders it totally immune to deformation caused by the application of the film-flattening vacuum (indeed, even the application of a hard vacuum will not alter its surface). The platen can accommodate up to 169 reseau projectors and has an rms flatness of well under 2 μm. The platen is shortly to be put forward as a standard product by DBA and will be offered for sale to interested parties.

LIKELY FUTURE DEVELOPMENTS

As the last few sections have indicated, the bundle adjustment with self-calibration can lead to considerable improvements in accuracies and can produce results helpful in pinpointing physical deficiences of the camera system. It is a safe prediction that the bundle adjustment with self-calibration will receive increasingly widespread attention over the next few years. A great deal of experimentation will inevitably be performed with various formulations of the error model (without doubt, spherical harmonics will be tried sooner or later). At DBA, for example, the original error model has been condensed and revised through practical experimentation (coupled with analytical considerations) to the following form:

$$\begin{aligned}\Delta x &= a_1x + a_2y + a_3xy + a_4y^2 + a_5x^2y + a_6xy^2 + a_7x^2y^2 \\ &+ \frac{x}{c}\left[a_{13}(x^2-y^2) + a_{14}x^2y^2 + a_{15}(x^4-y^4)\right] \\ &+ x\left[a_{16}(x^2+y^2)^2 + a_{17}(x^2+y^2)^4 + a_{18}(x^2+y^2)^6\right] \\ &+ a_{19} + a_{21}\left(\frac{x}{c}\right)\end{aligned} \tag{23}$$

$$\begin{aligned}\Delta y &= a_8xy + a_9x^2 + a_{10}x^2y + a_{11}xy^2 + a_{12}x^2y^2 \\ &+ \frac{y}{c}\left[a_{13}(x^2-y^2) + a_{14}x^2y^2 + a_{15}(x^4-y^4)\right] \\ &+ y\left[a_{16}(x^2+y^2)^2 + a_{17}(x^2+y^2)^4 + a_{18}(x^2+y^2)^6\right] \\ &+ a_{20} + a_{21}\left(\frac{y}{c}\right)\end{aligned}$$

In these expressions the first 12 coefficients are intended to account mainly for persistent, uncompensated film deformation together with non radial components of anomalous distortion. The coefficients of this particular subset are nearly orthogonal (i.e., their mutual correlations are mostly near zero) and are also nearly orthogonal to the next set of 6 coefficients. Of this next set, the first three (a_{13},a_{14},a_{15}) serve to represent the component of platen unflatness that is not strictly dependent on radial distance. They also serve to represent the radial component of anomalous distortion. When needed, an asymmetric contribution to platen unflatness is potentially available from the combined effect of the terms a_5x^2y and $a_{11}xy^2$ appearing in the first part of the error model. The coefficients a_{16},a_{17},a_{18} serve

to represent both residual symmetric radial distortion and the radially symmetric component of platen unflatness. Among the coefficients a_{13} through a_{18} a few moderately high correlations exist (from .85 to .97 for photos with a fairly uniform pattern of 25 measured points), but these are not sufficiently severe to induce ill-conditioning (even when a priori constraints are not exercised). The final coefficients a_{19},a_{20},a_{21} correspond to elements of interior orientation and are not normally exercised for reasons mentioned earlier. Specific coefficients for decentering distortion have not been carried in the above model because of their almost perfect coupling with other coefficients.

While experimentation with error modeling will continue for some time, so also will efforts to ascertain the usefulness of calibrations established from reductions of photographs taken over densely targeted aerial test fields. Such efforts are to be encouraged, for they can lead to better understanding of processes generating systematic error. In this respect, much more work needs to be done to establish the general significance of anomalous distortion. The isolation of anomalous distortion can be greatly facilitated if an ultra-flat reseau platen is employed.

Investigators employing test fields should adopt a highly critical and questioning attitude concerning the adequacy and accuracy of the ground survey. Analytical photogrammetry is fast approaching the stage where even the best of conventional surveys (of small test fields, in particular) may be inadequate. Special measures such as the use of direct and reverse runs along orthogonal flight lines should be considered to minimize the effects of both random and systematic errors in the control survey. Otherwise, emergent systematic effects ascribed to anomalous distortion could actually be caused by distortions in the control survey itself and have nothing to do with the camera.

Because the process of self-calibration has turned out to be so powerful and is not difficult to incorporate into the bundle adjustment, it seems unlikely that self-calibration will be displaced by precalibration. Improvements in accuracy by a factor of two to three seem now to be the general experience when self-calibration is exercised on blocks with moderate to sparse control. On the other hand, improvements are naturally much more modest in applications to small and relatively heavily controlled blocks as were investigated by Salmenperä, Anderson and Savolainen (1974).

The significance of self-calibration seems to be that it permits the bundle adjustment to approach its theoretical potential. Prior to the implementation of self-calibration it had been necessary to exercise an excessive amount of control in order to keep the systematic build-up of error within acceptable bounds. Now, with the implementation of self-calibration, the original promise of the bundle method can be realized — very large blocks can be safely and successfully adjusted with only a small fraction of the control required by previous standards. This can have enormous economic impact on large mapping projects in underdeveloped areas. It becomes practical, for instance, in remote and previously unsurveyed areas to employ the emerging technology of doppler surveying to establish with unprecedented speed, accuracy, and economy an integrated net adequate for the control of huge blocks (Brown (1975)).

As indicated earlier, the concept of self-calibration is not limited to the treatment of systematic errors in plate coordinates. As originally developed in Brown, Johnson and Davis (1964), it applied equally

to the output of any sensor producing observations serving ultimately to interrelate coordinates of photographed points. Parameters for self-calibration of external sensors of likely practical interest can be assigned to the border of the normal equations in just the same way as parameters for the self-calibration of the camera itself. As a result of the practical success reported by Ackermann (1974b) with the incorporation of observations made by a statoscope into the PAT-M-43 program for adjustment of independent models, it is logical that the statoscope be considered a prime candidate for similar incorporation into programs for bundle adjustment. A possibly worthwhile refinement of Ackermann's development might be the treatment of successive errors in statoscopic heights as being subject to a significant degree of serial correlation (as, indeed, they seem to be). If the serial correlation along each strip is considered to be governed by an autoregressive process, the rigorous adjustment of such errors in the bundle adjustment can be effected without disturbing the bandwidth of the normal equations. This is so even though the covariance matrix of the errors in statoscopic heights along each strip would be completely filled with nonzeroes, for, as pointed out in Brown and Trotter (1969), the inverse of such a covariance matrix is a banded matrix, the bandwidth being equal to $\ell+1$ where ℓ is the order of the autoregressive process. Hence, a more rigorous treatment of errors in statoscopic heights can be implemented without unduly burdensome consequences.

Another external sensor that is likely to emerge to prominence in the next few years is the inertial navigational system. Such a system has been adapted to applications to ground surveying with almost unbelievable success. It is produced by Litton Corporation under the trademark 'Autosurveyor'. Gregerson (1975) reports tests in which traverses were performed by the Autosurveyor to accuracies in excess of 1:100,000. The inertial navigator employed in the Autosurveyor is essentially the Litton LN-15, a unit developed in the mid 1960's and rated in accuracy at a little better than one nautical mile per hour in normal applications to aerial navigation. The state-of-the-art of inertial navigation has progressed to the point (see Figure 12 below) where accuracies of 0.08 nm/hr have been demonstrated in routine operations by the Honeywell SPN/GEANS (Standard Precision Navigation/Gimbaled Electrostatic gyro Aircraft Navigation System).

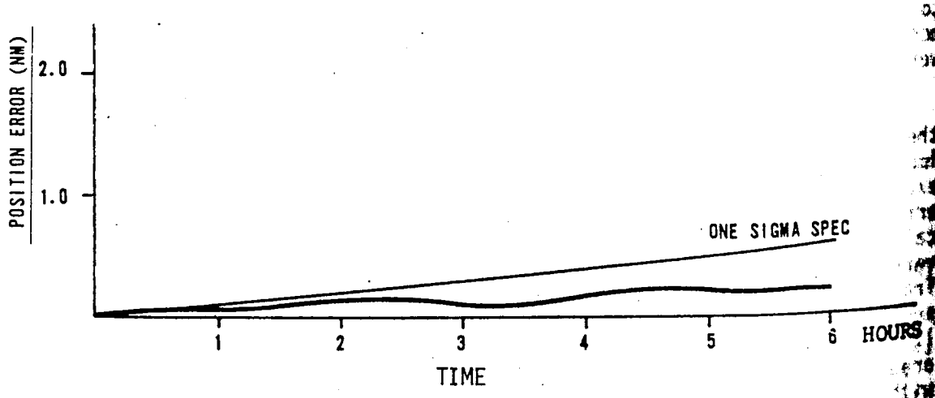

FIGURE 12. Error in aircraft positioning by Honeywell SPN/GEANS as determined from composite of nine laboratory tests (from Hall (1975)).

With SPN/GEANS the basic and relatively simple error model presented earlier in equation (21), supplemented perhaps in the bundle adjustment by an autoregressive treatment of stochastic errors, holds promise of suppressing residual build-up of positional error to a level of less than 1 meter per 100 kilometers. Accordingly, when the bundle adjustment with self-calibration is considered in conjunction with such rapidly developing technologies as doppler surveying and inertial navigation, the following scenario begins to emerge for the execution of very large mapping projects in the not-too-distant future. First, a basic, but sparse, control net is established to accuracies of 0.5 meters or better by doppler surveying — here, stations might well be spaced at 75 to 100 km intervals. Using the doppler stations as control points, an inertial surveying system is then employed to densify the doppler survey, particularly around the perimeter of the block to be flown (a spacing of 15 to 25 km along the perimeter might be appropriate for a photo scale of 1:50,000). An inertial system, most likely the very same unit as was used for first level densification of the doppler survey, is then mounted in the mapping aircraft in proximity to the aerial camera. Here, the unit functions both as a precise flight-line navigator and as an auxiliary sensor (perhaps along with a statoscope). In the latter capacity it provides a readout of inertial position corresponding to each photographic exposure. The coefficients of the error model of the inertial navigator (and statoscope) are then carried as strip-invariant parameters in the bundle adjustment along with error coefficients for the camera, which are carried as block-invariant parameters (or as sub-block invariant parameters, when more than one camera is employed to cover the block). Through the use of the inertial unit both on the ground and in the mapping aircraft, maximum economic benefits are realized from what might otherwise be a prohibitively expensive unit (at present, cost of a suitable unit with recommended spare parts approaches $500,000, but is likely to be reduced to less than half this amount by 1980).

Another development that may well have an impact on photogrammetric triangulation in the 1980's is the Global Positioning System (GPS). This system is being developed by the U.S. Air Force and will ultimately involve a total of 24 satellites so arranged that at least four suitably distributed satellites are to be visible at all times from all points on the earth. Simultaneous reception of signals from four satellites will enable a moving observer to determine his position in real-time to an absolute accuracy of 10 to 20 meters. With special refinements consisting mainly of the exploitation of doppler tracking and the use of appropriate error models in the bundle adjustment, the possibility exists for GPS to yield positions of the mapping aircraft to accuracies of a few decimeters. Here again, implementation of the process of self-calibration would lead to sets of strip-invariant error coefficients resident in the border of the normal equations.

Again and again reference is made in the foregoing discussions to the border of the banded-bordered system of normal equations. Without the border, the practical development of the bundle method would have remained essentially frozen at its status of a decade ago when recursive partitioning was first applied to the reduced normal equations. The border, more than anything else, provides the foundation for the recent development of the bundle method. To this point in the present discussion the border has been applied only to parameters in error models for the photographic coordinates or external sensors (or both). This is far from the limit of the utility of the border in photogrammetric adjustment. As shown in Brown (1974), the border can be exploited to introduce new information into the bundle adjustment without altering the essential character of the banded-bordered form of

the normal equations. One fully general approach designed specifically to accomplish this is the *method of augmented bordering* derived in Brown (1974). According to this method, new information implicit in the set of observational equations

$$\tilde{A}\tilde{v} + \tilde{B}\delta = \tilde{\varepsilon} \tag{24}$$

can be merged into an already existing set of banded-bordered normal equations

$$N\delta = c \tag{25}$$

through the following process of bordering:

$$\begin{bmatrix} N & \tilde{B}^T \\ \tilde{B} & -(\tilde{A}\tilde{\Lambda}\tilde{A}^T) \end{bmatrix} \begin{bmatrix} \delta \\ \tilde{\delta} \end{bmatrix} = \begin{bmatrix} c \\ \tilde{\varepsilon} \end{bmatrix} . \tag{26}$$

Here, $\tilde{\Lambda}$ denotes the covariance matrix of the observations appearing in the new system of observational equations (24) and $\tilde{\delta}$ is a vector of s new parameters, where s denotes the number of new equations introduced by (24). Inasmuch as the matrix N is already postulated to be of banded-bordered form, it follows that the new system (26) is also of such form with the borderwidth of N being augmented by s new elements. Thus the method of augmented bordering permits one to introduce new information in a manner that preserves the banded-bordered characteristics of the basic system of normal equations.

Through the method of augmented bordering and other strategems aimed at exploiting the border, it becomes possible to generate practical solutions to a variety of special photogrammetric problems that would otherwise be cumbersome or intractable. A number of these are specifically addressed in Brown (1974) and will only be mentioned here:

(a) *the rigorous simultaneous adjustment of both photogrammetric and geodetic observations (two different approaches leading to banded-bordered normal equations are developed);*

(b) *the introduction of equal-elevation constraints arising from measurements along shorelines of lakes, some of which may span many models (each lake utilized adds one element to the border and has no effect on the bandwidth);*

(c) *the introduction of orbital constraints into strips or blocks of photographs taken by a satellite borne camera (full details are to be found in Haag and Hodge (1972));*

(d) *accommodation of datum shifts between different geodetic nets connected by a common photogrammetric block;*

(e) *accommodation of parameters of relative orientation of multiple cameras rigidly fixed with respect to one other (e.g., as with multispectral systems or with stellar-oriented terrain cameras);*

(f) *accommodation of parameters for self-calibration of photographic measurements and/or external sensors (repeated here for the sake of completeness).*

The actual implementation of practical applications of the fully generalized bundle adjustment is far from complete and can draw for years to come from the broad theoretical base already in place.

REFERENCES

Ackermann, F., 1974a. *Results of Recent Experimental Investigations in Aerial Triangulation.* Presented to the 40th Annual Meeting of the American Society of Photogrammetry, St. Louis, March 10-15, 1974.

Ackermann, F., 1974b. *Accuracy of Statoscope Data - Results from the OEEPE-Test "Oberschwaben".* Paper presented to the Symposium in Stuttgart, sponsored by Commission III of the International Society for Photogrammetry, Sept. 2-6, 1974.

Bauer and Müller, 1972. *Height Accuracy of Blocks and Bundle Adjustment with Additional Parameters.* Presented to the Twelfth Congress of the International Society for Photogrammetry, Ottawa, July-Aug. 1972.

Brown, D.C., 1958. *A Solution to the General Problem of Multiple Station Analytical Stereotriangulation.* RCA-MTP Data Reduction Technical Report No. 43, Patrick Air Force Base, Florida (also designated as AFMTC TR 58-8).

Brown, D.C., 1959. *Results in Geodetic Photogrammetry I: The Precise Determination of the Location of Bermuda from Photogrammetric Observations of Flares Ejected from Juno II.* RCA-MTP Data Reduction Technical Report No. 54, Patrick Air Force Base, Florida (also designated as AFMTC TR 59-25).

Brown, D.C., 1968a. *A Unified Lunar Control Network.* Presented at the 34th Annual Convention of the American Society of Photogrammetry, Washington, D.C., March 1968. Also published in Photogrammetric Engineering, Dec. 1968.

Brown, D.C., 1968b. *Inversion of Very Large Matrices Encountered in Large Scale Problems of Photogrammetry and Photographic Astrometry.* Presented at the Conference of Photographic Astrometric Technique, University of South Florida, Tampa, Florida, March 1968. Also published in NASA CR-1825: Conference on Photographic Astronomic Technique, November 1971.

Brown, D.C., 1968c. *Advanced Methods for the Calibration of Metric Cameras.* Final Report prepared for U.S. Army Engineering Topographic Laboratories, Fort Belvoir, Va., under U.S. Army Contract No. DA-44-099-AMC-1457X. Also presented to the 1969 Symposium on Computational Photogrammetry, Syracuse University, Syracuse, N.Y., January 1969.

Brown, D.C., 1971. *Close-Range Camera Calibration.* Presented at the Symposium on Close-Range Photogrammetry, University of Illinois, Urbana, Illinois, January 1971. Also published in Photogrammetric Engineering, Aug. 1971.

Brown, D.C., 1972. *Calibration of Close Range Cameras.* Presented at the XII Congress of the International Society of Photogrammetry, Ottawa, Canada, July-Aug.1972.

Brown, D.C., 1973. *Accuracies of Analytical Triangulation in Applications to Cadastral Surveying.* Presented at the 1973 Annual Meeting of the American Congress of Surveying and Mapping, Washington, D.C., March 1973. Also published in Surveying and Mapping, September 1973.

Brown, D.C., 1974. *Evolution, Application and Potential of the Bundle Method of Photogrammetric Triangulation.* Presented to the Symposium in Stuttgart, sponsored by Commission III of the International Society for Photogrammetry, September 2-6, 1974.

Brown, D.C., 1975. *A Primer on Satellite Doppler Surveying.* DBA Technical Note 75-002.

Brown, Davis, Johnson, 1964. *The Practical and Rigorous Adjustment of Large Photogrammetric Nets.* RADC TRD-64-092, Rome Air Development Center, Rome, N.Y.

Davis, R.G., 1965. *Analytical Adjustment of Large Blocks.* Presented at the 31st Annual Meeting of the American Society of Photogrammetry, Washington, D.C., March 1965. Also published in Phogorammetric Engineering, Jan. 1966.

Gregerson, L.F., 1975. *Inertial Geodesy in Canada.* Paper presented at the Meeting of the American Geophysical Union in San Francisco, December 8-10, 1975.

Gyer, M.S., 1967. *The Inversion of the Normal Equations of Analytical Aerotriangulation by the Method of Recursive Partitioning.* RADC-TR-67-69. Rome Air Development Center, Rome, New York.

Gyer, Lewis, Saliba, 1967. *Mathematical Targeting III.* RADC-TR-67-562. Rome Air Development Center, Rome, NY.

Haag, Hodge, 1972. *Analysis for the Photogrammetric Lunar Orbital Data Processing System.* Final Report prepared for the U.S. Army Engineer Topographic Laboratories, Fort Belvoir, Virginia, under U.S. Army Contract Nos. DACA76-70-C-003 and -004.

Hall, P.E., 1975. *Gimbaled Electrostatically Suspended Gyro Aircraft Navigation System.* Paper presented to the Ninth Joint Services Data Exchange for Inertial Systems, 19 November 1975, and published as Report No. 1175-13426, Honeywell Aerospace Division, St. Petersburg, Florida.

Kenefick, J.F., 1971. *Ultra Precise Analytics.* Presented at the Symposium on Close Range Photogrammetry, University of Illinois, Urbana, Illinois, January 1971. Also published in Photogrammetric Engineering, November 1971.

Salmenperä, Anderson, Salvolainen, 1974. *Efficiency of the Extended Mathematical Model in Bundle Adjustment.* Presented to the Symposium in Stuttgart, sponsored by Commission III of the International Society for Photogrammetry, Sept. 2-6, 1974. Also published in BuL, 229-233,1974.

Sechler, E.E., 1968. *Elasticity in Engineering.* Dover Publications, New York.